



<https://rbgeomorfologia.org.br/>  
ISSN 2236-5664

## Revista Brasileira de Geomorfologia

v. 26, n° 2 (2025)

<http://dx.doi.org/10.20502/rbg.v26i2.2623>



Research article

# Five decades of morphological evolution and hydro-sedimentary interactions in a fluvial confluence in the Brazilian Cerrado

*Cinco décadas de evolução morfológica e interações hidrossedimentares em uma confluência fluvial no Cerrado brasileiro*

Pâmela Camila Assis<sup>1</sup>, Márcio Henrique de Campos Zancopé<sup>2</sup>, Luan Ferreira Siqueira<sup>3</sup>, Hudson de Azevedo Macedo<sup>4</sup>, and Maximiliano Bayer<sup>5</sup>

<sup>1</sup> Universidade Federal de Goiás (UFG), Programa de Pós-Graduação em Ciências Ambientais (CIAMB), Goiânia, Brasil. pcassis@discente.ufg.br.

ORCID: <https://orcid.org/0000-0001-6526-6780>

<sup>2</sup> Universidade Federal de Goiás (UFG), Instituto de Estudos Socioambientais (IESA), Goiânia, Brasil. zancope@ufg.br.

ORCID: <https://orcid.org/0000-0002-9778-4301>

<sup>3</sup> Universidade Federal de Goiás (UFG), Programa de Pós-Graduação em Ciências Ambientais (CIAMB), Goiânia, Brasil. siqueiraluan93@hotmail.com.

ORCID: <http://orcid.org/0000-0003-3524-960X>

<sup>4</sup> Universidade Federal de Mato Grosso do Sul (UFMS), Faculdade de Engenharias, Arquitetura e Urbanismo e Geografia (FAENG), Campo Grande, Brasil. hudson.macedo@ufms.br

ORCID: <https://orcid.org/0000-0003-1104-7106>

<sup>5</sup> Universidade Federal de Goiás (UFG), Instituto de Estudos Socioambientais (IESA), Goiânia, Brasil. maxbayer@ufg.br.

ORCID: <https://orcid.org/0000-0002-0873-0564>

Received: 01/10/2024; Accepted: 24/04/2025; Published: 13/06/2025

**Abstract:** River confluences are zones of intense hydro-sedimentary interaction whose morphological dynamics remain poorly understood in tropical environments, especially in the Cerrado biome. This study investigates the morphodynamic transformations at the confluence of the Araguaia and Vermelho Rivers in Aruanã (Goiás, Brazil), over 51 years (1972–2023). The study integrates remote sensing data, bathymetry, and acoustic profiling. Riverbanks, thalwegs, sandbars, junction angle, and channel width were mapped, along with the calculation of hydraulic and geomorphological parameters. The results reveal high planimetric mobility, with junction displacement of up to 2.5 km, a 27° reduction in the confluence angle, and intense fluctuations in the configuration and area of fluvial bars. The confluence was characterized by a retreat between the 1970s and 2000 due to the erosion of part of the floodplain; then an advance of the confluence was observed in the period from 2000 to 2023, driven by formation and consolidation of the tributary bar. The dominance of the Araguaia River influences the scour zone position and thalweg configuration. Differential bank erosion was observed, conditioned by the morpho-sedimentary units of the floodplain, as well as colonization of the tributary bar by vegetation, promoting temporary stabilization. It is concluded that the adjustments in the confluence morphology result from an interaction between the seasonal hydro-sedimentary regime, bank lithology, and migration of fluvial forms, highlighting a dynamic system that is sensitive to changes in land use and land cover.

**Keywords:** Araguaia River; Fluvial Geomorphology; ADCP; Bathymetry.

**Resumo:** As confluências fluviais são zonas de intensa interação hidrossedimentar, cuja dinâmica morfológica permanece pouco compreendida em ambientes tropicais, especialmente no bioma Cerrado. Este estudo investiga as transformações morfodinâmicas na confluência dos rios Araguaia e Vermelho, em Aruanã (Goiás), ao longo de 51 anos (1972–2023). A pesquisa integra dados de sensoriamento remoto, batimetria e perfilação acústica. Foram mapeadas margens, talvegues, barras arenosas, ângulo de junção e largura do canal, além do cálculo de parâmetros hidráulicos e geomorfológicos. Os resultados evidenciam alta mobilidade planimétrica, com deslocamento da junção em até 2,5 km, redução de 27° no ângulo de confluência e intensas oscilações na configuração e área das barras fluviais. Entre as décadas de 1970-2000, a confluência foi caracterizada por um recuo, resultante da erosão de parte da planície, no período de 2000-2023, observou-se um avanço da confluência, impulsionado pela formação e consolidação da barra do tributário. A dominância do rio Araguaia influencia a posição da zona de escavação e a configuração do talvegue. Verificou-se a atuação da erosão diferencial das margens, condicionada pelas unidades morfossedimentares da planície, e a colonização por vegetação na barra de tributário, promovendo estabilizações temporárias. Conclui-se que os ajustes na morfologia da confluência resultam da interação entre o regime hidrossedimentar sazonal, a litologia das margens e a migração de formas fluviais, evidenciando um sistema dinâmico e sensível às alterações no uso e cobertura da terra.

**Palavras-chave:** Rio Araguaia; Geomorfologia Fluvial; ADCP; Batimetria.

## 1. Introduction

Channel confluences (also known as river junctions), are environments of complex interactions between matter (water and sediment) and energy. They present continuous changes in flow structure (discharge, velocity, direction), channel morphology and sediment transport (bed load and suspended load), with particular and exclusive biophysical processes of great importance for the river ecosystem (MILLER, 1958; BEST, 1987; BEST, 1988; BEST; ROY, 1991; RICE et al., 2008).

River channel junctions play an important role from an ecological point of view, as they are the site of complex biophysical interactions, provide valuable ecosystem services, and contain a rich biodiversity of fauna and flora, converging in a unique environment (RICE et al., 2008). They especially respond to significant changes in flow dynamics, sediment transport, and bed morphology which occur along the river basin (RIBEIRO et al., 2012). River channel confluences were considered neglected components of river systems in the past (BEST, 1986). However, the geomorphological processes that occur at channel junctions have been considered of relevant scientific interest in recent decades. This is because the fluvial and morphological processes in these environments represent the main characteristics of river basins, while also playing an important role in regulating water and sediment circulation in the downstream drainage network (SANTOS; STEVAUX, 2017).

The research field on channel confluences began in the 1970s and has since gained increasing momentum and recognition in the context of fluvial studies. The contributions of Mosley (1976) and Best (1988) stand out, whose investigations primarily focused on geomorphology and sedimentology. In addition, the studies of Mosley (1976), Best (1987), and Roy et al. (1988) focused on the hydraulics and hydrology of channel confluences, while studies by Petts (1984), Bruns et al. (1984) and Petts and Greenwood (1985) played an important role in the ecology of fluvial junctions. Drainage structure assessment was addressed by Abrahams and Campbell (1976), Flint (1980) and Abrahams and Updegraph (1987). These contributions have consolidated over time and enriched understanding of channel confluence in the panorama of river studies (STEVAUX; LATRUBESSE, 2017).

The Cerrado saw a reduction of approximately 27% of its native vegetation between 1985 and 2023, while areas designated for agriculture currently occupy 47% of its extension according to data from the Mapbiomas Project, collection 9 (SOUZA et al., 2020). This dynamic of land use and occupation has led to classifying the biome in recent decades as “severely threatened” (SILVA, 2020). Recent studies indicate that advancement of the agricultural frontier over the last five decades in the Araguaia River basin has resulted in intense conversion of natural areas to pastures and soybean, corn and sugarcane crops (CASTRO, 2005; BAYER et al., 2020; GOMES et al., 2022; ASSIS et al., 2025). The region underwent significant changes in land use and coverage between 1985 and 2022, with a significant reduction in the Forest Formation (-44.21%), Savanna Formation (-41.53%) and Grassland Formation (-34.74%). On the other hand, there was a sharp increase in Pasture areas (+148.73%), and mainly Soybean (+1581.19%) (ASSIS et al., 2025).

This conversion process altered the volume of sedimentary load transported and deposited in the Araguaia River channel, producing significant geomorphological and hydrological changes (LATRUBESSE et al., 1999;

BAYER, 2002; LATRUBESSE; STEVAUX, 2002; MORAIS, 2006; AQUINO et al., 2008; LATRUBESSE et al., 2009; COE et al., 2011; BAYER, 2010; BAYER; ZANCOPÉ, 2014; ZANCOPÉ et al., 2015; BAYER et al., 2020; SUIZU et al., 2022; SANTOS et al., 2024). The total set of transformations made the Araguaia one of the largest sediment storage and transport areas in the Cerrado (LATRUBESSE et al., 2009; BAYER, 2010). These transformations directly influenced the morphometric parameters and geomorphological elements of the river-plain system (number of islands, type of bars, sinuosity, width/depth ratio, among others). Clear trends in the geomorphological response of the Araguaia River system to changes in use and cover were detected when analyzed and compared from the records of the last four decades (BAYER; ZANCOPÉ, 2014; BAYER et al., 2020; SANTOS et al., 2024).

Although research has found marked morphological changes and an abrupt increase in sediments along the Araguaia River in recent decades (LATRUBESSE et al., 2009; BAYER et al., 2020; ASSIS; BAYER, 2020, SUIZU et al., 2022; SANTOS et al., 2024), little is known about the effects on the confluences with their tributaries. Therefore, this study aims to understand the main morphological changes at the river confluence between the Araguaia and Vermelho Rivers in the city of Aruanã (GO, Brazil), based on the planimetric displacement of channel geoforms obtained by chronological sequence of satellite images and hydrodynamic and bathymetric data obtained by Acoustic Doppler Current Profiler (ADCP). This is the first study on river confluences in Cerrado environments that integrates ADCP, echo sounder and remote sensing data. It is also worth considering the environmental, social and economic importance of this river basin for the Cerrado (BAYER et al., 2020), and that the abrupt increase in sediments in recent decades has the potential to cause several changes in the hydro-sedimentary parameters in the river channel (LATRUBESSE et al., 2009), mainly resulting in morphological changes in the confluence stretches.

## 2. Study area

The Araguaia River originates in the Serra do Caiapó, near the Emas National Park, in the southwest of the state of Goiás in central Brazil. It runs for approximately 2,600 km until it meets the Tocantins River (ANA, 2015), encompassing parts of the states of Goiás, Mato Grosso, Tocantins and Pará. The Araguaia River basin covers an area of over 386,000 km<sup>2</sup> (ANA, 2015). According to Latrubesse and Stevaux (2002), the Araguaia River is divided into three segments: upper, middle and lower Araguaia. The stretch of the Araguaia River analyzed in this study is located in the middle section of the river, specifically a 5 km long segment covering the junction with the Vermelho River, a tributary on the right bank (Figure 1), adjacent to the city of Aruanã in the state of Goiás. The Araguaia River runs for approximately 605.23 km up to the point of the river junction, and the Vermelho River, which originates in the Serra Geral in the city of Goiás, runs for 300.96 km. The Vermelho River basin has a drainage area of approximately 11,000 km<sup>2</sup> (SEMAD, 2011), which represents approximately 2.85% of the entire Araguaia River basin.

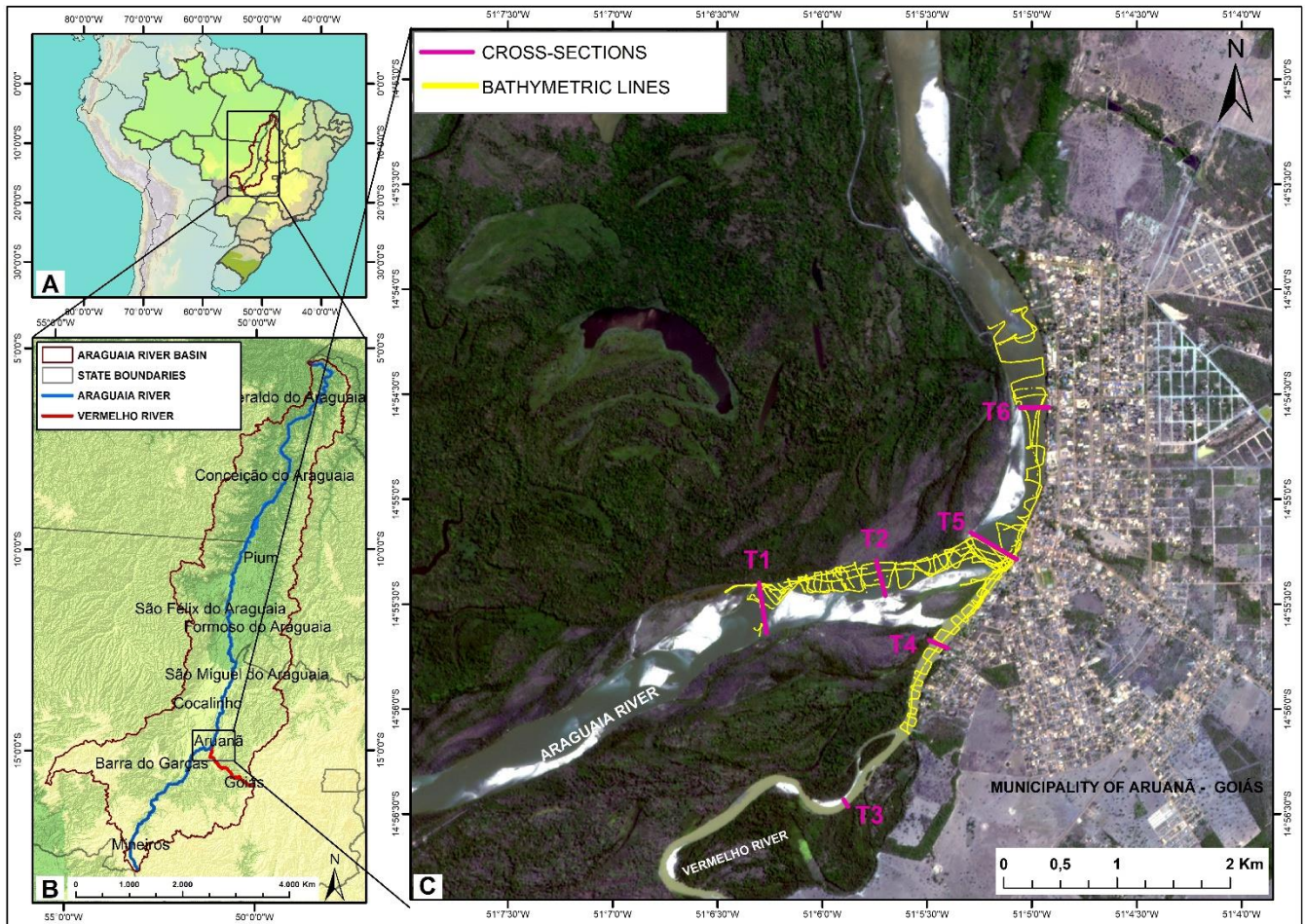


**Figure 1.** A – Location of the Araguaia River basin in Brazil. B - Location of the Araguaia River basin. C - Location of the confluence of the Araguaia and Vermelho Rivers. Landsat/OLI image from October 20, 2023, color composite R(4)G(3)B(2). Databases: IBGE/MMA/ANA/ANADEM. Source: The authors, 2025.

The Araguaia River basin mainly drains mixed terrains dominated by platforms formed by Paleozoic and Mesozoic sedimentary basins, in addition to cratonic areas, which represent the Precambrian crystalline basement (LATRUBESSE et al., 2005). The basin is composed of three main geological units: Precambrian rocks, Paleozoic and Mesozoic rocks of the Paraná Basin, and Neogene-Quaternary deposits in the Bananal Plain (LATRUBESSE; STEVAUX, 2002; VALENTE; LATRUBESSE, 2012).

The upper Araguaia River runs embedded in a crystalline basement formed by Precambrian rocks and Paleozoic sediments from the Paraná sedimentary basin (AQUINO et al., 2009). It flows through a well-developed alluvial plain in the middle stretch which forms a complex mosaic of morpho-sedimentary units, mainly composed of sediments from the Holocene and Late Pleistocene periods (AQUINO et al., 2009). This plain is segmented into three main morpho-sedimentary units (Units I, II and III) according to Bayer (2002) and Latrubesse and Stevaux (2002), with the right bank of the Araguaia River in the study area delimited by sediments of the Araguaia Formation. Unit I is the oldest, and covers areas with impeded flow in the most distant and lower parts of the plain. Unit II is the highest and most predominant, is located between Units I and III, and is characterized by the presence of paleomeanders and oxbow lakes. Unit III is composed of a complex of bars and islands, which reflect the current morphodynamics of the alluvial system.

Specific dating analyses for the Araguaia Formation indicate that the sedimentary process associated with this formation was particularly significant during the Middle and Upper Pleistocene periods, occurring approximately between 240,000±29,000 and 17,200±2,300 years BP (before present), as reported by Valente and Latrubesse (2012). The alluvial plain presents a continuous linear configuration in this section of the Araguaia River, integrated with the Plio-Pleistocene sediments related to the Araguaia Formation. This geological formation is composed of a variety of alluvial sediments, including sandy-conglomeratic, sandy and silty-clayey, with the latter partially

ferruginized (VALENTE; LATRUBESSE, 2012).

Grain size and morphometric analyses in the Araguaia and Vermelho River confluence region showed significant differences in the characteristics of the collected sediments (OLIVEIRA, 2021). The Araguaia River samples were collected in a side bar upstream of cross-section T1 (Figure 1) at points located in the center of the bar and on the edge. The central sample of the bar presented more than 60% of the sediments in the medium fraction, while the edge sample exhibited a balanced distribution between the medium sand and coarse to very coarse sand fractions. The sediments of both samples were predominantly composed of grains classified as well-rounded in both granulometric fractions, followed by rounded grains, with a percentage of less than 20%.

Additionally, a high percentage of grains classified in the “very good” roundness class was observed. Two Vermelho River samples were collected from a sand bar in cross-section T3 (Figure 1), one at the edge and the other at the center of the bar. The sample from the bar edge predominantly presented sediments in the medium sand fractions, with approximately 15% of fine sand and coarse to very coarse sand, while the central sample revealed a similar distribution between the fine and medium sand fractions. The sediments of these samples were also mostly classified as well rounded, with between 15% and 25% of the sediments in the subangular and rounded classes. As in the Araguaia River, the Vermelho River sediments also demonstrated a predominance of grains with a “very good” roundness degree. When comparing the roundness index of the samples, it was observed that the Vermelho River sediments presented a lower degree of roundness compared to those of the Araguaia River, indicating that the Araguaia grains have a higher degree of maturity (OLIVEIRA, 2021).

Aquino et al. (2009) identified that the cross-section referenced in this study as T6 (Figure 1) has a bed predominantly composed of medium and coarse sand. Available data on the concentration of suspended sediments (C<sub>ss</sub>) in this section reveal values that vary between 21.7 mg·L<sup>-1</sup> and 181.4 mg·L<sup>-1</sup> (Aquino et al., 2009). However, no studies to date have been recorded which address C<sub>ss</sub> values in the Vermelho River.

The climate in the Araguaia River basin follows the typical pattern of the Cerrado biome, classified as type Aw according to the Koppen climate classification system, with two clearly defined seasons: a rainy season from October to April and a dry season from May to September. This alternation results in significant variations in river flow, with peaks during the rainy season and a reduction in the dry months (Figure 2). This dynamic is conditioned by factors such as precipitation, geology, and geomorphology of the region (AQUINO et al., 2005; LATRUBESSE and STEVAUX, 2002).

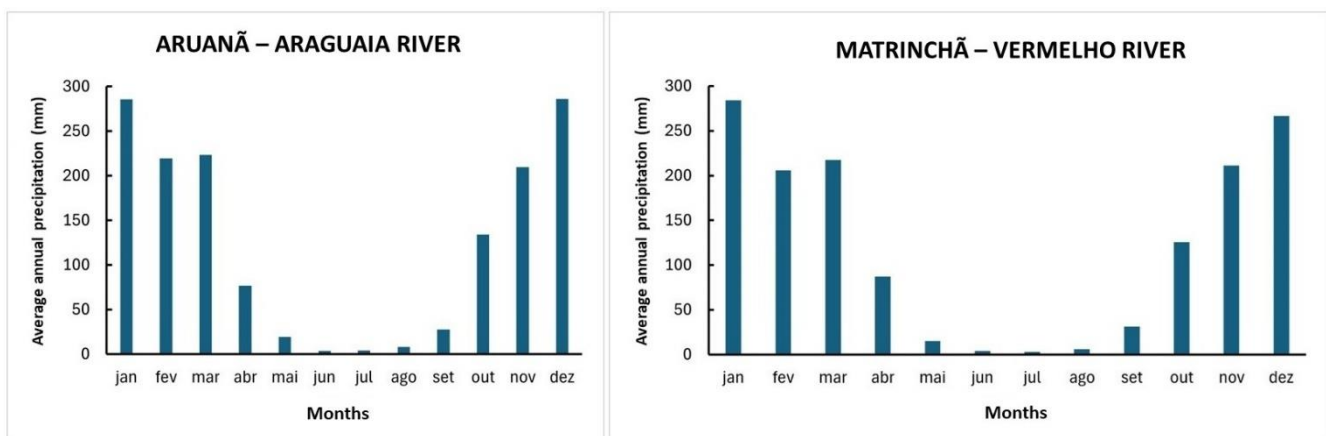


**Figure 2.** Fluviometric stations of Aruanã on the Araguaia River (Code: 25200000) from 1970 to 2024, and of Matrinchã on the Vermelho River (Code: 25130000) from 1974 to 2024. Source: The authors, 2025.

Based on data available on the Hidroweb Platform (operated by CPRM-ANA), the flows recorded at the Aruanã station located on the Araguaia River show significant variations throughout the hydrological cycle, ranging from approximately 2,500 m<sup>3</sup>·s<sup>-1</sup> during the flood period to approximately 350 m<sup>3</sup>·s<sup>-1</sup> in the dry season, from 1970 to 2023 (Figure 3). The levels at this station exhibit an annual variation amplitude of approximately 150 cm. Similarly, the average flows at the Matrinchã station on the Vermelho River for the period from 1974 to 2021 reach values around 180 m<sup>3</sup>·s<sup>-1</sup> during the flood period, decreasing to approximately 20 m<sup>3</sup>·s<sup>-1</sup> in the dry season. The elevations at the Matrinchã station show an even more pronounced variation, around 200 cm, reflecting the

seasonal dynamics characteristic of the region. The station located in Matrinchã was chosen to represent the Vermelho River because it is the closest to the confluence, located approximately 74 km from the study area.

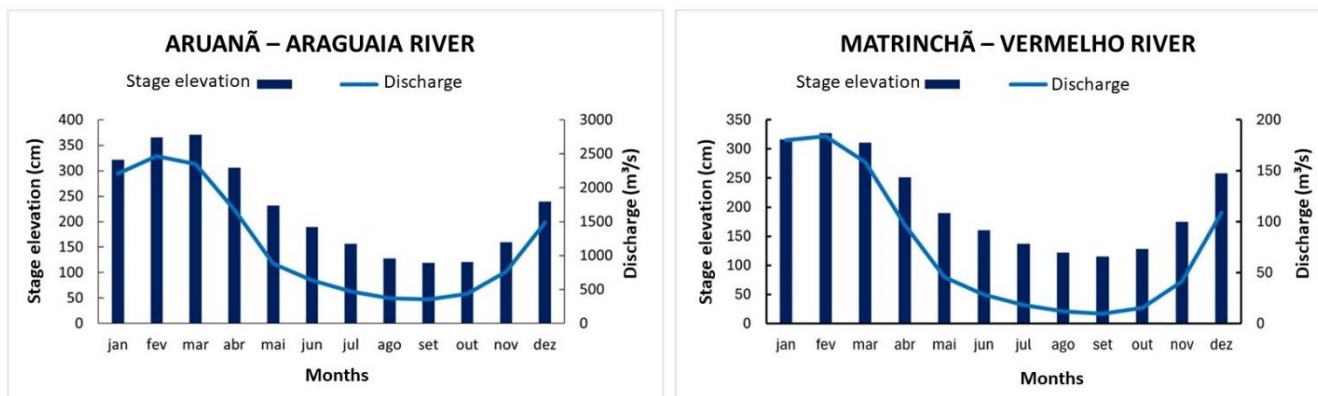


**Figure 3.** Fluviometric stations of Aruanã on the Araguaia River (Code: 25200000) from 1970 to 2023, and of Matrinchã on the Vermelho River (Code: 25130000) from 1974 to 2021. Source: The authors, 2025.

These data demonstrate the hydrological variability of the Araguaia and Vermelho Rivers, reflecting the natural oscillations of the hydrological cycle in the Cerrado environment. The amplitude of the flows and levels recorded in both stations highlights the importance of considering these variations in the analysis of river dynamics and in understanding the geomorphological processes at the confluences of this river. In this context, it is important to install a monitoring station on the Vermelho River in a location closer to the confluence in order to provide more precise and representative data on the hydrological conditions directly in the study area.

### 3. Methods

Planimetric mapping based on the delineation of the banks, thalwegs and sand bars was performed for a detailed analysis of the morphodynamic behavior of the confluence. Satellite images from the Landsat series, available on the United States Geological Survey (USGS) platform, for the period from 1972 to 2023 were used for this purpose. Image selection was based on the lowest flow levels recorded during the dry season, which range from 129 to 180 cm. Sedimentary deposits become more evident in the river channel under these conditions, which facilitates a more precise analysis and reduces the possibility of errors in delimiting morphological elements, such as bars, which may be partially emerged or submerged, depending on the river stage.

Appendix 1 compiles the dates, elevations and flows corresponding to the selected images, with additional notes in the caption that clarify the criteria for selecting the images. Thus, it was possible to map the geomorph displacement of 44 images (44 years) in the 51-year time scale considered. The remaining years/images were discarded due to an absence of images which met the criteria for mapping, such as being within the quota interval, or because they presented visual obstructions (smoke or clouds) or displacements.

The selected Landsat images were visually interpreted and using the ArcGIS/ArcMap software at a scale of 1:5,000, with manual vectorization of the fluvial geomorphs performed according to the methodology described by Morais (2006). Thus, the sand bars were categorized based on their location in the fluvial channel as central bars, lateral bars and tributary bars (BEST; RHOADS, 2008) (Figure 4).

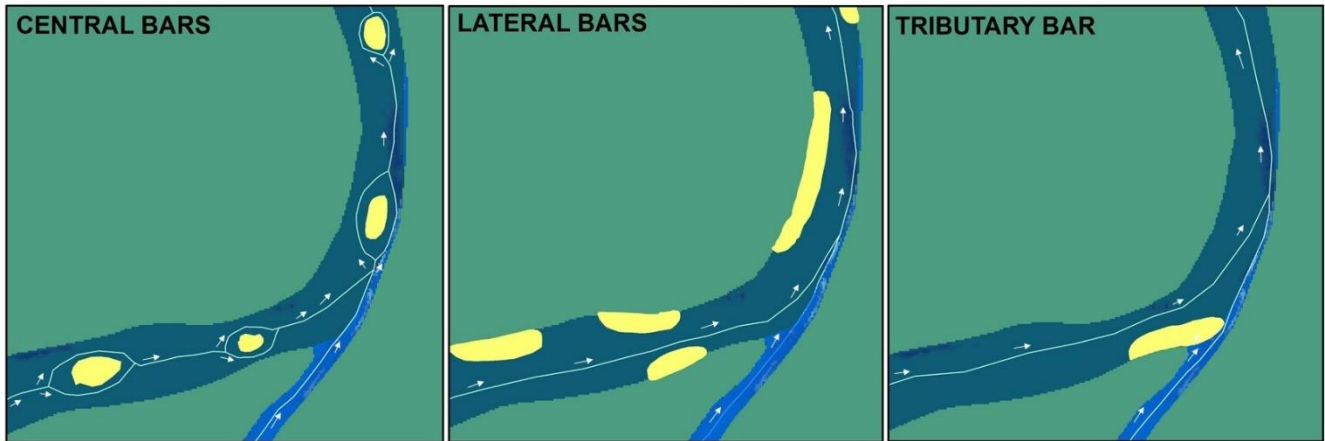


**Figure 4.** Representation of central and lateral bars and tributary bars based on their location in the river channel. Source Adapted from Best; Rhoads (2008). Prepared by: The authors, 2025.

Next, photographs and aerial images obtained during fieldwork were used to better visualize the morphological features of the confluence. Images were captured at a height of 120 m with a DJI Mavic 3 aerial platform equipped with a standard RGB digital camera (20 megapixels) provided by the Image Processing and Geoprocessing Laboratory (Lapig/UFG).

In turn, geoprocessing techniques were applied using the ArcGIS/ArcMap 10.3 program to calculate the morphometric parameters, such as the number and area of sand bars, channel width, erosion and deposition area, and the thalweg sinuosity index. Editing tools in ArcMap were used to manually draw polygons around the sand bars. The eroded or accreted margin areas were delimited between the previous position of the margin (1972) and the subsequent position (2023). If the margin retreated over the plain, there was a loss of area; if the bank advanced over the channel (with consolidation of vegetation), there was lateral accretion. A decadal analysis using a bar graph was performed to better understand the areas of deposition and erosion.

The width of the cross-sections (T1, T2, T3, T4, T5 and T6; Figure 1) were measured in the field on October 28, 2023. Based on these sections, it was possible to measure the width of the river stretches between 1972 and 2023. The Müller Parameter (Eq. 1) was adopted to calculate the thalweg sinuosity index, which is an approach recognized for its effectiveness in evaluating this index, as cited by Friend and Sinha (1993), Ghosh and Mистри (2012), and Nimnate et al. (2017).

$$I_s = C_{max}/C_v \quad (1)$$

in which:  $C_{max}$  is the length of the channel or thalweg, and  $C_v$  is the length of the valley along the channel, in a straight line.

The data on the thalweg sinuosity index were analyzed for the period 1972 to 2023 using the classification proposed by Morisowa (1975). This classification categorizes river channels as straight (index <1.05), sinuous (>1.05), braided (>1.3), meandering (>1.5) and anastomosing (>2.0).

The methodology used to measure the confluence angle follows the approach proposed by Hackney and Carling (2011). The center lines of the rivers were initially drawn, and then the angle formed at the intersection of these lines was measured. The confluence angle was measured using spatial analysis tools in QGIS (angle measurement), and integrated satellite images with the mapping of the banks, thalweg and sand bars mapped in previous steps.

Next, a detailed refinement of the morphosedimentary units of the alluvial plain close to the municipality of Aruanã, Goiás, was performed to improve understanding of the planimetric transformations at the confluence. This stage was based on previous studies by Bayer (2010), Bayer and Zancopé (2014) and Suizu et al. (2022). The employed methodology involved using images from the Landsat-8 satellite, captured on October 27, 2023 (date which allowed the data to be associated with the fieldwork, described below). In addition, there was a review process of the geological vector data prepared by the Geological Survey of Brazil (*Serviço Geológico do Brasil - SGB/CPRM*) and made available by the National Water Agency (*Agência Nacional de Águas - ANA*). This review

phase included a more detailed definition of the limits for the classes related to the Araguaia Formation and the Alluvial Deposits, which contributed to more refined understanding of the characteristics and dynamics of the studied area.

Data on river flow, velocity, width and depth were measured in the field using a WorkHorse Rio Grande 600 kHz Acoustic Doppler Current Profiler (ADCP, Teledyne RD Instruments), provided by the Laboratory of Geomorphology, Pedology and Physical Geography of the Federal University of Goiás (Labogef/UFG). The internal compass of the ADCP was juxtaposed to the external Global Navigation Satellite System (GNSS) for calibration with the dual-frequency Geodetic GNSS receiver (Trimble, Model R4) and data recording. The equipment was attached to the side of a vessel and positioned 20 cm below the waterline. The ADCP was connected to a laptop with WinRiver II software (version 2.08) using the Bottom Tracking reference during the operation, which automatically calculated the measured variables, returning the average value of the cross-sections. The fieldwork was conducted on October 28, 2023, and profiled six transects (T1 to T6).

In the same campaign, the SONAR HELIX 7 X MSI WITH GPS - SCREEN 7.0 G4 from Labogef/UFG was used to obtain bathymetric lines with intervals of 50 m to 100 m. This interval was adopted due to obstructions such as tree branches or very shallow areas, among others. The generated points were exported in shapefile format and interpolated using the natural neighbor algorithm of ArcGIS/ArcMap 10.3 to the SIRGAS2000 geodetic reference system. The data obtained by ADCP and bathymetry enabled calculating the discharge ratio ( $Q_r$ ), Eq. (2) and the momentum ratio ( $M_r$ ) of the confluence between the Araguaia and Vermelho Rivers. According to Best (1987), these two hydraulic parameters classify the control of flow structures and morphology in confluence environments regarding the dominance of the main river (receiver) over the tributary (affluent) or vice versa, as:

$$Q_r = Q_t / Q_p \quad (2)$$

in which:  $Q_t$  is the flow rate of the tributary channel and  $Q_m$  is the flow rate of the main channel. When  $Q_r < 1$ , there is dominance of the flow of the receiving channel; and when  $Q_r > 1$ , the dominance is of the tributary.

The momentum ratio ( $M_r$ ) is given by Eq. (3):

$$M_r = (\rho_t Q_t V_t) / (\rho_p Q_p V_p) \quad (3)$$

in which:  $\rho$  is the fluid density,  $Q$  is the mean discharge and  $V$  is the mean velocity; and  $M_r < 1$  indicates the dominance of the main channel flow at the confluence, and  $>1$  the dominance of the tributary (BEST, 1987; SERRES et al., 1999).

Then, the channel power (stream power) and the specific channel power, as defined by Bagnold (1960, 1966), were calculated in order to evaluate the energy contribution of the Araguaia and Vermelho River flows at the confluence. The concept of channel power ( $\Omega$ ) (Equation 4), given in the unit of  $W \cdot m^{-1}$ , makes the relationship between channel energy and slope even clearer.

The calculation of channel power ( $\Omega$ ) was performed using the Eq. (4):

$$\Omega = \rho g D Q \quad (4)$$

in which:  $\Omega$  = channel power;  $\rho$  = Water density ( $1,000 \text{ kg/m}^3$ );  $g$  = Acceleration of gravity ( $9.81 \text{ m/s}^2$ );  $D$  = Slope (dimensionless);  $Q$  = Flow rate ( $\text{m}^3 \cdot \text{s}^{-1}$ ).

In turn, the average depth of each section was assumed as the bed elevation to calculate the slope, considering that the waterline level remains constant between sections. Thus, the equation takes the form:  $(Dep2 - Dep1)/Dis$ , where  $Dep$  represents the depth and  $Dis$  is the distance. It is observed that  $\rho$  and  $g$  are normally considered constants, whose product gives rise to the specific weight of the water. In this case, the energy of a river channel mainly varies as a function of the slope and the flow rate.

Then by dividing  $\Omega$  by the width of a cross section ( $w$ ), Bagnold (1960, 1966) defined the average energy available per unit area of the channel bed ( $\omega$ ). The specific power ( $\omega$ ) of the channel was subsequently calculated using Eq. (5):

$$\omega = \Omega / w \quad (5)$$

in which:  $\omega$  = specific channel power ( $W \cdot m^{-2}$ ),  $\Omega$  = channel power;  $w$  = channel width (m).

The hydrological data from the fluvimetric stations of Aruanã (#25200000) covering the period from 1970 to 2023, and Matrinchã (#25130000) from 1974 to 2021, were obtained through the HidroWeb Portal (<http://www.snirh.gov.br/hidroweb>), maintained by the National Water Agency (ANA).

#### 4. Results

##### 4.1. Dynamics of the banks, thalweg and river bars

Planimetric mapping of the Araguaia and Vermelho River confluence was performed in 44 years over a period of 51 years (1972-2023) due to the availability of satellite images from the Landsat series. The results revealed a high mobility of the confluence characterized by significant changes in the banks, thalweg, angle, width and sand bars, evidencing its instability and constant morphological reconfiguration (Figure 5). A total of 1.19 square kilometers (km<sup>2</sup>) were eroded between 1972 and 2023, while 0.92 km<sup>2</sup> were gained by accretion. The superposition of the bank, thalweg and contour lines of the sand bars (Figure 5 – A', B' and C', respectively), reveals the most frequent positioning of these morphological elements, and whose oscillation delimits what can be considered the mobile bed of the Araguaia.

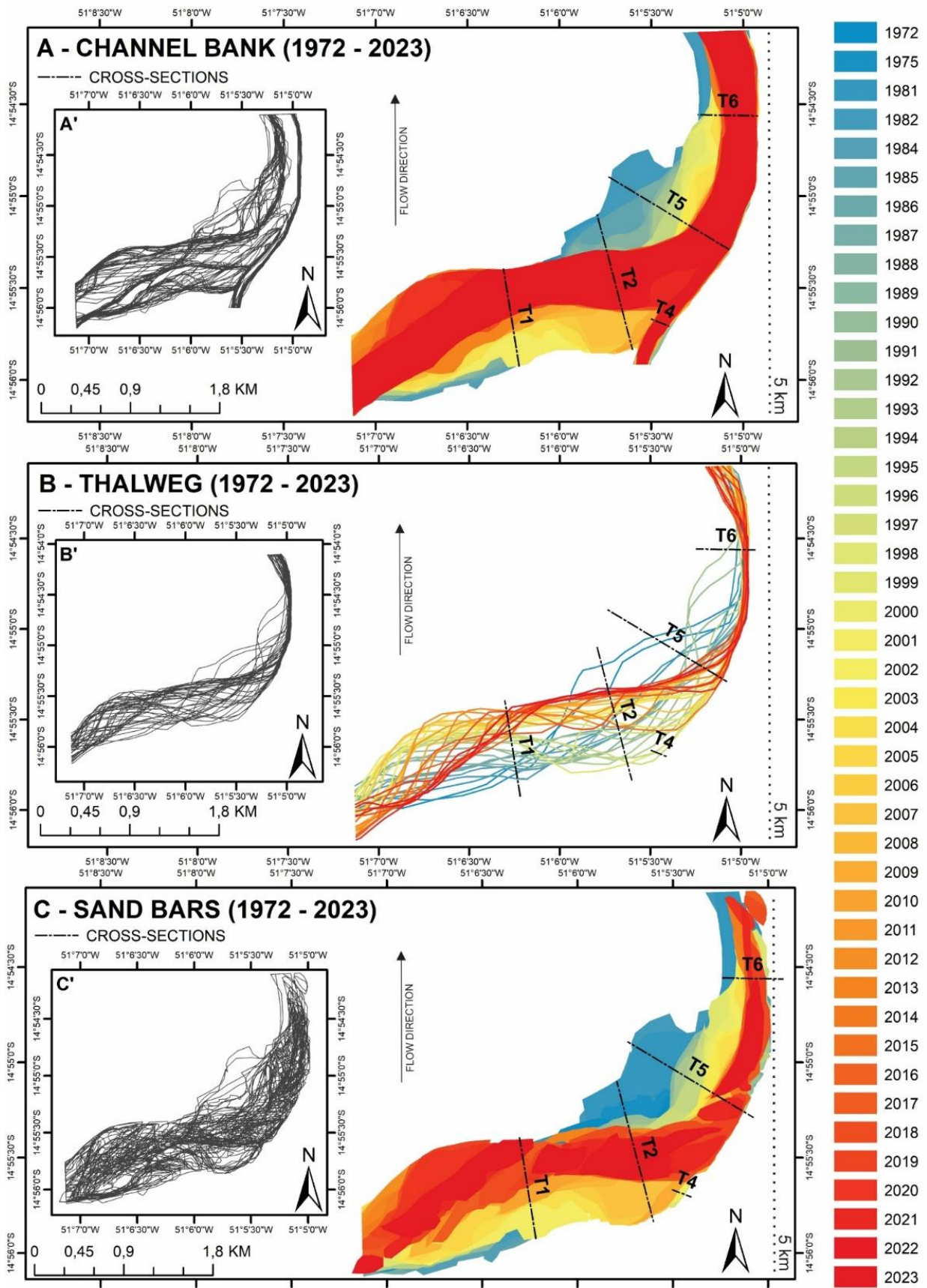
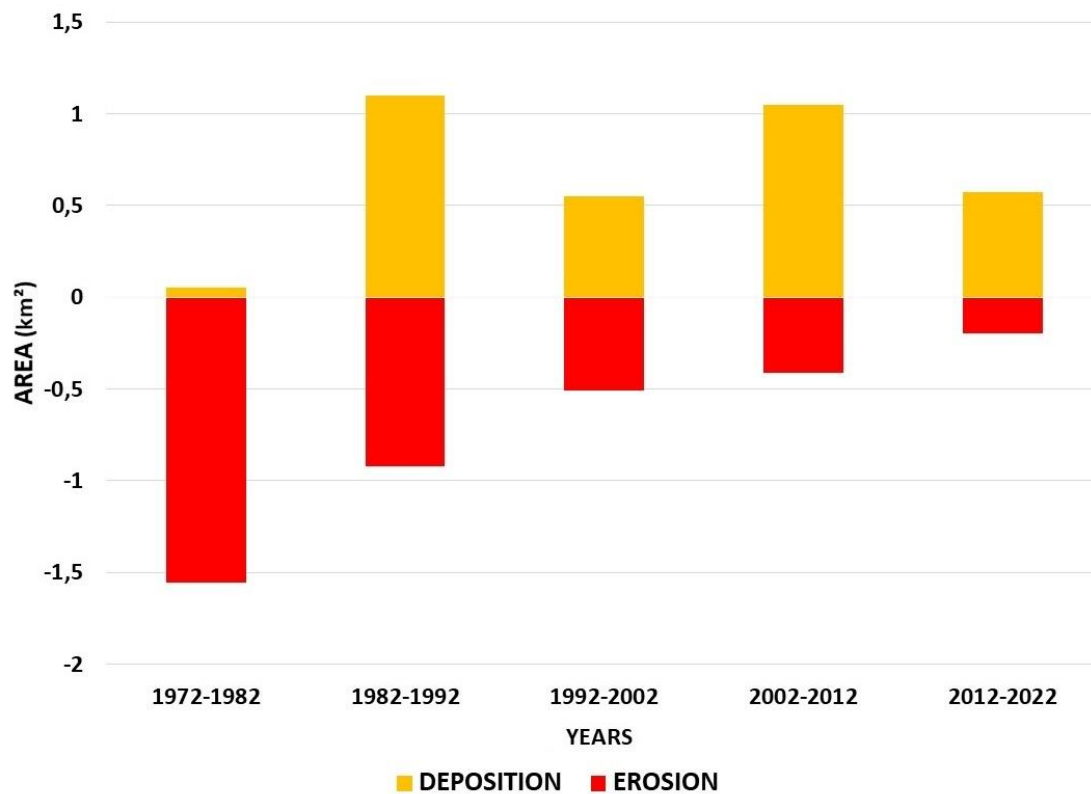


Figure 5. Mapping of the banks, thalweg and sand bars from 1972 to 2023 at the Araguaia and Vermelho River confluence in 2023. Source: The authors, 2025.

In analyzing the annual rates over this 51-year period, erosion occurred at an average rate of 0.023 km<sup>2</sup>-year<sup>-1</sup> and accretion occurred at an average rate of 0.018 km<sup>2</sup>-year<sup>-1</sup>, resulting in a continuous and gradual repositioning of area. There was a gain in area due to accretion, but the loss due to erosion was greater. A decadal analysis (Figure 6) shows varied sediment balance, observing that there was a relatively low deposition of 0.05 km<sup>2</sup> and a lateral erosion of 1.55 km<sup>2</sup> from 1972 to 1982, marking this interval as the one of greatest erosion in the decades analyzed.

In contrast, the period from 1982 to 1992 showed a reversal in this trend, with deposition reaching its greatest volume, 1.09 km<sup>2</sup>, while erosion decreased to 0.92 km<sup>2</sup>. Deposition between 1992 and 2002 was 0.55 km<sup>2</sup> and erosion continued to decrease, reaching 0.50 km<sup>2</sup>. Deposition increased again to 1.05 km<sup>2</sup> in the period from 2002 to 2012, while erosion continued to decline, reducing to 0.41 km<sup>2</sup>. Finally, deposition in the last decade analyzed (from 2012 to 2022) was 0.57 km<sup>2</sup> and erosion reduced further to 0.19 km<sup>2</sup>, the lowest rate recorded in all periods studied (Figure 6).



**Figure 6.** Erosion and deposition from 1972 to 2022 at the Araguaia and Vermelho River confluence in 2023. Source: The authors, 2025.

It was observed that the sand bars played a modeling role in configuring the confluence in the studied area. The years 2013 and 2021 stood out for presenting the largest number of sand bars throughout the mapping period (Figure 7).

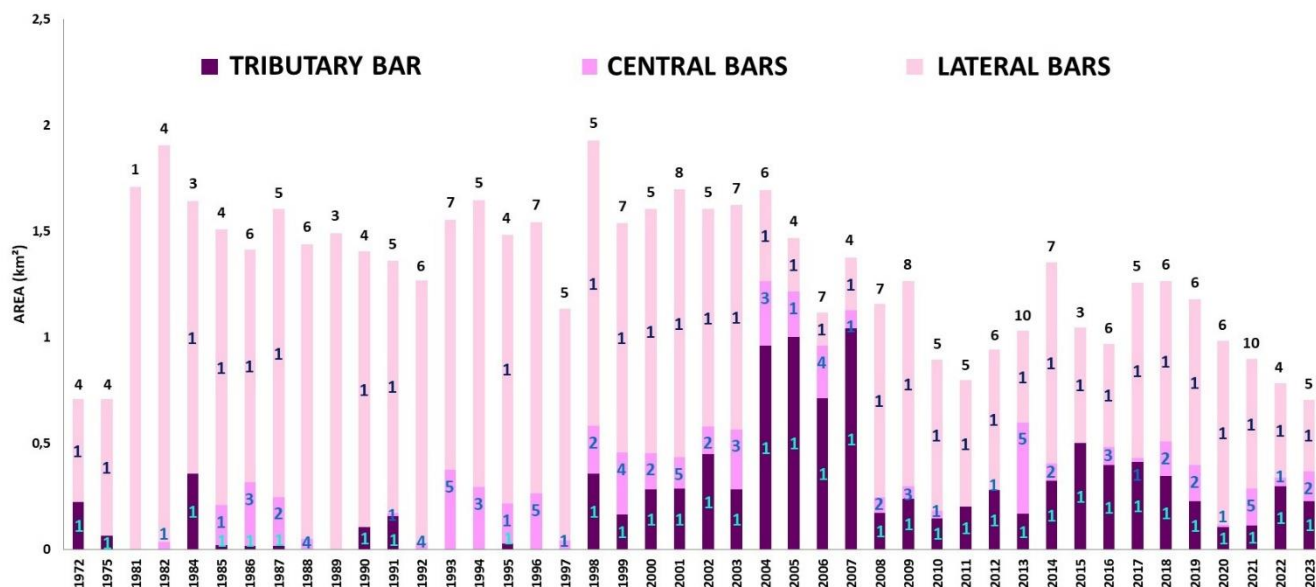


**Figure 7.** Variation of sand bars from 1972 to 2023 at the Araguaia and Vermelho River confluence. The numbers at the top of the columns correspond to the total number of bars per year, while the numbers inside the columns correspond to the total number of each type of bar per year. Source: The authors, 2025.

On the other hand, 1981 recorded the lowest quantity with only one lateral bar of approximately 1.70 km<sup>2</sup>. Lateral bars were the most prevalent type of bars in terms of area and quantity compared to central bars and tributary bars over the years. A significant increase was recorded in the total area of lateral bars between 1972 and 1982, which expanded from 0.48 km<sup>2</sup> to 3.57 km<sup>2</sup>. However, after peaking in 1982, the total lateral bar area began to decline, reaching 2.88 km<sup>2</sup> in 1988. The lateral bar area continued to fluctuate from then until 2023, showing an overall decreasing trend, reaching a minimum of 0.33 km<sup>2</sup> in 2023.

The tributary bar area also showed significant changes, with some years missing (1981, 1982, 1988, 1989, 1992, 1993, 1994, 1996 and 1997). The most notable year was 2007, when the area reached 1.04 km<sup>2</sup>. However, there was a sharp variation after that year in the total areas of the tributary bars with a continuous downward trend, resulting in a decrease to 0.23 km<sup>2</sup> in 2023. The period from 1981 to 1993 was marked by a gradual growth in regarding the central bar area, reaching 0.37 km<sup>2</sup> in 1993. The areas then remained relatively stable between 1993 and 2013, with an increase to 0.43 km<sup>2</sup> in 2013. However, a downward trend in the area was observed after 2013, which reduced to 0.14 km<sup>2</sup> in 2023.

4.2. Oscillation of the junction point, thalweg sinuosity and angular variation at the confluence

Mapping the junction point between the Araguaia and Vermelho Rivers combined with delimiting the banks allowed us to verify the pendular oscillation of the river junction (Figure 8), with alternating advances and retreats annually, demonstrating the unstable nature of the confluence. Appendix 2 compiles data regarding the thalweg sinuosity index, the junction angle and the channel width in the cross-sections for the period from 1972 to 2023. It was possible to quantify a significant change in the confluence position between 1972 and 2023, with a maximum variation of up to 2.5 km (Figure 8).

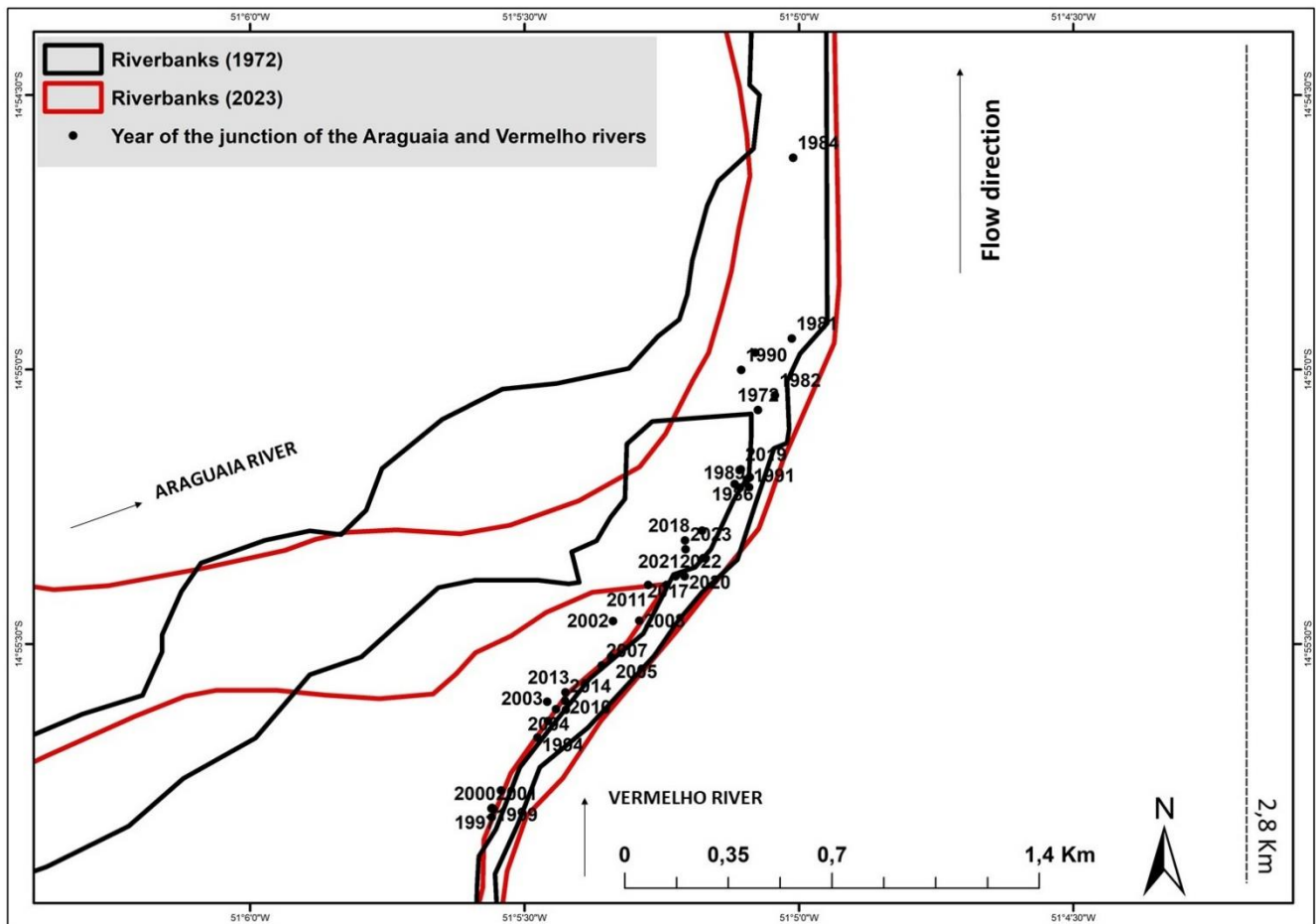


**Figure 8.** Changes in the junction location of the Araguaia and Vermelho Rivers from 1972 to 2023. Source: The authors, 2025.

The time series analysis of the Araguaia River thalweg sinuosity index from 1972 to 2023 reveals significant variations over time (Figure 9-A). Starting with an index of 1.162 in 1972 and reaching 1.209 in 2023, the maximum value was recorded in 1998, with 1.311. Other notable peaks occurred in 1999, 2007 and 2014, with indices of 1.305, 1.281 and 1.284, respectively, while the minimum value was observed in 1981, with 1.134. There was a significant drop in the index between 1999 and 2000, with the same variability which began in 1991 being recovered from 2003 onwards. Based on the classification by Morisowa (1975), the annual indices exceeded the value of 1.05, confirming the continuous sinuous pattern throughout the analyzed period. The sinuosity indices reached 1.311 and 1.305 in 1998 and 1999, respectively (Figure 9 - A).

The confluence junction angles also varied significantly (Figure 9-B), from a minimum of 30° in 1984 to a maximum of 94.22° in 1996, evidencing a high variation amplitude. This variation suggests complex river dynamics with periods of substantial changes in the confluence configuration. Notable peaks were observed in 2010 (93.75°), 1997 (78.75°), 2003 (75.58°), 2004 (75.53°) and 1995 (73.6°). Relative stability is evident during the period from 1981 to 1994, with angles predominantly between 30° and 48°. The angles continued to vary between 42.3° and 75.58° in more recent years, from 2000 to 2023. The studied confluence predominantly maintained an acute angle throughout these 44 years of mapping, meaning less than 90°, except in two specific years of 1996 and 2010, when obtuse angles of 94.22° and 93.75° were recorded, respectively (Figure 9-B).

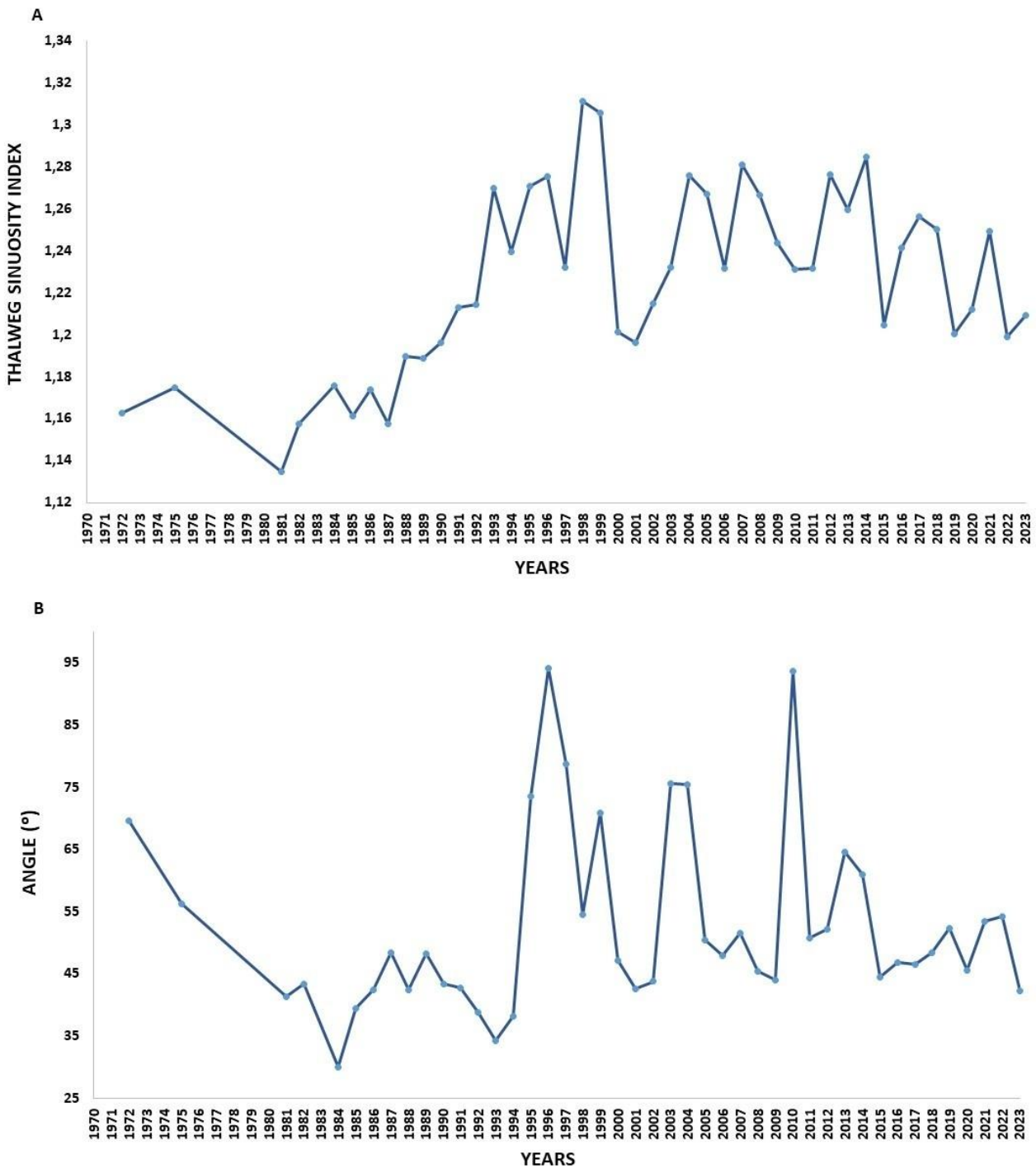


**Figure 9.** Thalweg sinuosity index (A) and angle (B) between 1972 and 2023 at the Araguaia and Vermelho River confluence. Source: The authors, 2025.

*4.3 Analysis of cross-sections and hydraulic parameters in the confluence zone*

The excavation zone, the tributary bar and the lateral bar stand out among the main morphological characteristics observed at the Araguaia and Vermelho River confluence. The excavation zone begins at the mouth of the Vermelho River and extends along the Araguaia River bed for approximately 600 meters, with depths varying between 3 and 5.2 meters. It is also noted that this zone presents repositioning and migration tendencies over time within the main channel (Figure 10).

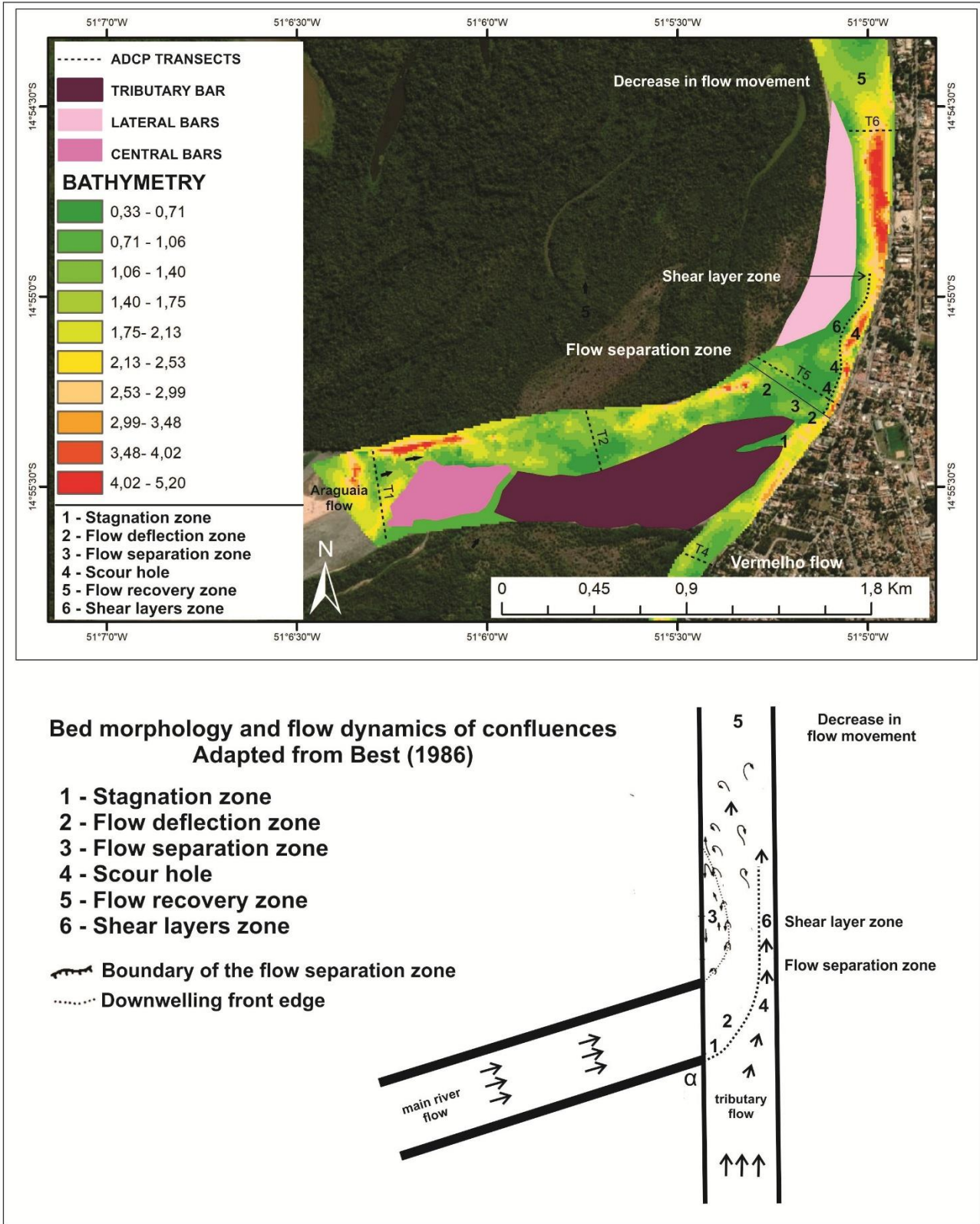


**Figure 10.** Description of the morphological characteristics at the Araguaia and Vermelho River confluence in 2023. Source: The authors, 2025.

The previous data revealed marked mobility between the different types of sand bars, as well as the river junction throughout the studied period. Morphological parameters were verified in six cross-sections (T1 to T6) in order to distinguish the influence of each river on the confluence dynamics, as located in figures 1 and 5.

The variables of the respective parameters were surveyed in the same low-water period of the annual seasonal river regime, maintaining methodological compliance. All cross-sections showed high variability for the channel width, mainly from 1980 onwards (Figure 11), except for section T3 (further upstream of the Vermelho River).

Section T1, which had a width of 301 m in 1972, experienced a series of fluctuations over the years, reaching a peak of 462 m in 2023. The minimum value recorded was 95 m in 2013, highlighting a notable amplitude of variation over the years. In turn, section T2 started at 558 m in 1972 and exhibited considerable instability, reaching a peak of 844 m in 2000 and declining to a minimum of 101 m in 2017; then, it was recorded at 309 m in 2023. In contrast, section T3 maintained generally low values, starting at 88 m in 1972 and decreasing to 48 m in 2023. The reduction in width in this section was due to the formation of a sand bar, classified as a point bar, as described by Oliveira (2021). The maximum width value recorded in section T3 was 89 m in 1987, while the minimum was 37 m in 2005, evidencing a more contained variation compared to the other sections. Section T4, which was 140 m in 1972, reduced its width to 110 m in 2023. Section T5, which was 461 m in 1972, peaked at 815 m in 2010 and a minimum of 250 m in 1994, and in 2023, it was 425 m wide. Finally, section T6 started at 123 m in 1972, peaked at 526 m in 1996, and was 208 m wide in 2023.

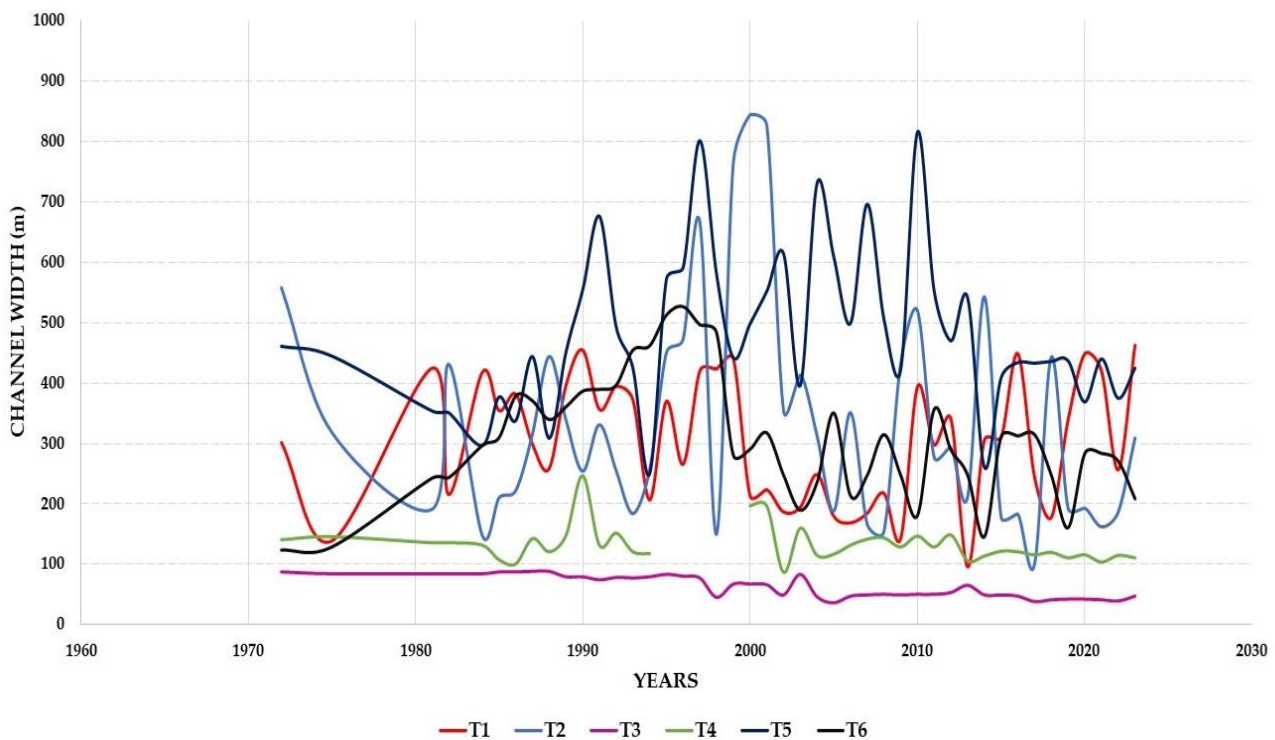


**Figure 11.** Changes in width at T1, T2, T3, T4, T5 and T6 cross-sections from 1972 to 2023 at the Araguaia and Vermelho River confluence. Source: The authors, 2024.

In addition to the morphological data, hydraulic variables were also obtained in the respective cross-sections using an ADCP. It was observed that the Araguaia River presented a flow rate of  $202.99 \text{ m}^3\cdot\text{s}^{-1}$  in section T1, and the Vermelho River presented  $8.45 \text{ m}^3\cdot\text{s}^{-1}$  in T3 (both upstream of the confluence), with an increase after the confluence reaching  $243.01 \text{ m}^3\cdot\text{s}^{-1}$  in T6. The Araguaia River flow rate is substantially higher, approximately 24 times greater, than the flow recorded for the Vermelho River, demonstrating a large difference in the water volume between the receiving channel and the tributary during the dry season for these cross-sections.

Next, the width values were 391.74 m, 38.18 m and 163.09 m, for T1, T3 and T6, respectively. When comparing the data in Table 1 and Figure 12, it can be seen that the maximum depths reached were 3.49 m, 3.69 m and 5.54 m in the same T1, T3 and T6 sections, respectively. The flow rate at the confluence in section T5 was  $245.04 \text{ m}^3\cdot\text{s}^{-1}$ , with a width of 422.49 m, a velocity on the left bank (Araguaia River) of  $0.585 \text{ m}\cdot\text{s}^{-1}$  and on the right bank (Red

River) of  $0.382 \text{ m}\cdot\text{s}^{-1}$ , with the excavation zone (Figure 10) reaching a depth of 5.2 m. The Araguaia River thalweg after the excavation zone and the beginning of the flow recovery zone is well defined on the right river bank.

**Table 1.** Flow data, width, boat speed, speed and flow direction at the Araguaia and Vermelho River confluence.

Section	$Q_{\text{Total}} \text{ (m}^3\cdot\text{s}^{-1}\text{)}$	Width (m)	Flow speed $\text{(m}\cdot\text{s}^{-1}\text{)}$	Mean depth (m)	Flow direction (°)	Water temperature (°C)
T1	202.99	391.74	0.352	1.46	35.11	31.2
T2	184.87	290.40	0.623	1.01	109.84	31.6
T3	8.45	38.18	0.095	2.34	45.89	33.3
T4	32.29	118.68	0.185	1.46	45.07	32.9
T5	245.04	422.49	0.447	1.73	69.06	32.7
T6	243.01	163.09	0.479	3.15	358.26	32.9

Source: The authors, 2025.

Figure 12 shows the distribution of current velocities along the profile of the respective cross-sections during the same low-water period. Cross-section T1 showed two deeper sectors at the ends of the profile, which may be associated with the thalweg position change in the Araguaia River. The thalweg was located on the right side of the river in 2022. However, the 2023 data obtained by the ADCP and by mapping remote sensing images indicate a change in the thalweg position to the left bank. It is also worth noting that the Vermelho thalweg is still present immediately downstream of the junction in section T5, with predominantly lower velocities than those of the much shallower Araguaia.

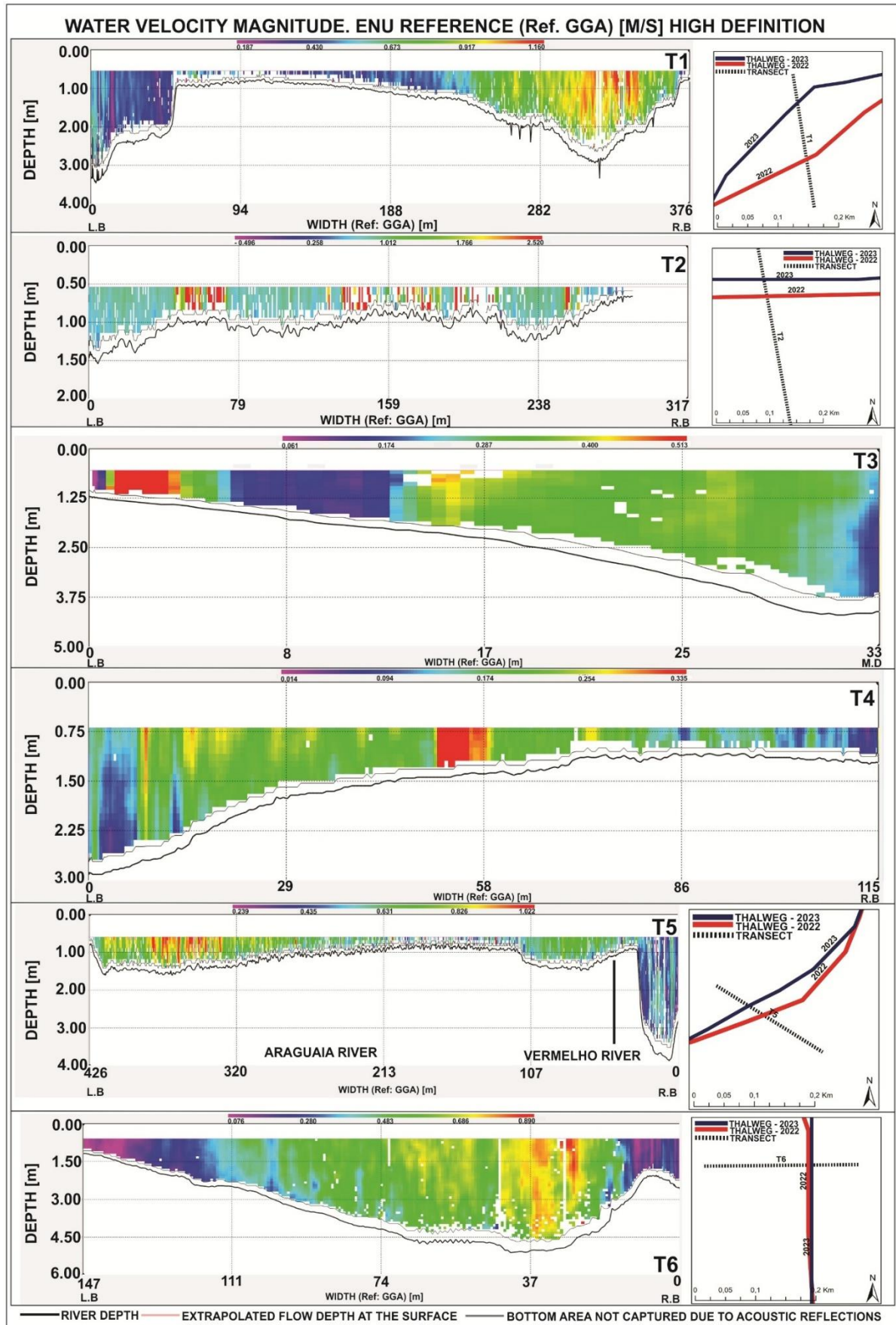


**Figure 12.** Magnitude of water velocity in the T1, T3, T5 and T6 sections. LB – Left Bank and RB – Right Bank. Source: The authors, 2025.

The hydraulic variables also enabled calculating the discharge ( $Qr$ ) and momentum ( $Mr$ ) ratios to assess the dominance of one river over another at the confluence (BEST, 1987; SERRES et al., 1999). These parameters were applied to the T2 and T4 sections because they are located at the river junction (Table 2). A  $Qr$  of 0.174 was obtained, which means that the Vermelho River flow represents approximately 17.4% of the Araguaia River flow. Concomitantly, the  $Mr$  of 0.051 indicates that the Vermelho River contributes approximately 5.1% of the total. These  $Qr$  and  $Mr$  values demonstrate the dominance of the Araguaia River (receiving channel) over the Vermelho tributary during the low-water period.

**Table 2.** Discharge ratio ( $qr$ ), momentum ratio ( $mr$ ), channel power and specific channel power of the Araguaia and Vermelho Rivers.

Sections	Flow	Width	Slope	$Qr$	$Mr$	$\Omega$	$\omega$
Araguaia (T2)	184.87	290.40	0.0004261			772.76	2.66
				0.174	0.051		
Vermelho (T4)	32.29	118.68	0.000534			169.15	1.42

Source: The authors, 2025.

Then, the channel powers ( $\Omega$ ) and specific channel powers ( $\omega$ ) were determined for the same T2 and T4 sections. In addition to being located at the river junction, they had sections T1 and T3 as a reference for calculating the slope in this river segment to determine  $\Omega$  and  $\omega$ . The  $\Omega$  and  $\omega$  values calculated for the Araguaia River were  $772.76 \text{ J}\cdot\text{s}^{-1}$  and  $2.66 \text{ W}\cdot\text{m}^{-2}$ , and for the Vermelho River they were  $169.15 \text{ J}\cdot\text{s}^{-1}$  and  $1.42 \text{ W}\cdot\text{m}^{-2}$ , as shown in Table 2. These values indicate that the main river is receiving a significant energy contribution from its tributary. In addition, they demonstrate the superior capacity of the Araguaia River to perform erosive and sediment transport activities (as well as other geomorphological transformations) when compared to the Vermelho River.

## 5. Discussion

### 5.1. Morphological mobility and reconfiguration of sandbanks and bars

Studies on river confluences in Brazil are still incipient, and little is known about the hydrogeomorphological changes in these environments and the possible changes that may occur over time, such as lateral adjustments caused by erosion and deposition, changes in the typology of sand bars and their reconfiguration within the channel, in the advance and retreat of the junction, in the excavation zone and in angle changes.

The analysis presented in this study for the Araguaia and Vermelho River confluence is in line with the studies by Kominecki and Vestena (2021), which highlight the vulnerability of river confluences in alluvial plains to changes caused by sedimentary characteristics and climatic conditions. Wang and Xu (2020) suggest that alluvial rivers may present more progressive dynamics at their confluences. Our results on the Araguaia-Vermelho confluence converge with the observations of Dixon et al. (2018), who point out that confluences located in areas with high sediment supply rates, high flows and easily erodible banks tend to be highly mobile due to the migration of bars which modify the orientation and location of the channels, promoting displacement of the confluences.

The combination of several hydromorphic and sedimentary elements in these environments is essential for the channel's morphological evolution over time. Factors such as climate variations, water seasonality and the basin's geological characteristics directly influence the quantity and quality of sediments transported and deposited by the river. In addition, changes in land use and cover can further impact this sedimentary dynamic by modifying surface runoff, intensifying soil erosion and altering the sediment load which reaches the river channel, as pointed out by Latrubesse et al. (2009), Bayer (2010) and Bayer et al. (2020) for the case of the Araguaia River.

The planimetric evolution of the confluence of the Araguaia and Vermelho Rivers suggests that it is influenced by these changes in land use and cover that occur in the basin, which consequently alter the hydrosedimentary characteristics, and by the facies characteristics of the materials which compose the banks. The high mobility of the

banks, thalweg, sand bars and changes in the junction angle and position identified in this study are the result of these morphological elements repositioning on the unconsolidated sediments of Morpho-Sedimentary Unit III, which remains geomorphologically active, continually shaping the alluvial plain, as observed by Bayer (2002). However, this mobility is contained by the Araguaia Formation on the right bank (Figure 13).

The Araguaia Formation had a significant sedimentary process particularly associated with the Middle and Upper Pleistocene, between 240,000±29,000 and 17,200±2,300 B.P. (VALENTE; LATRUBESSE, 2012). It is composed of a variety of alluvial sediments (Figure 17 - D), and is significantly more resistant to erosion processes. Thus, the geological characteristics influence the distribution of sand bars, the thalweg mobility in the river channel and changes in the junction angle, which can both intensify and mitigate erosion processes, significantly impacting river morphology over time.

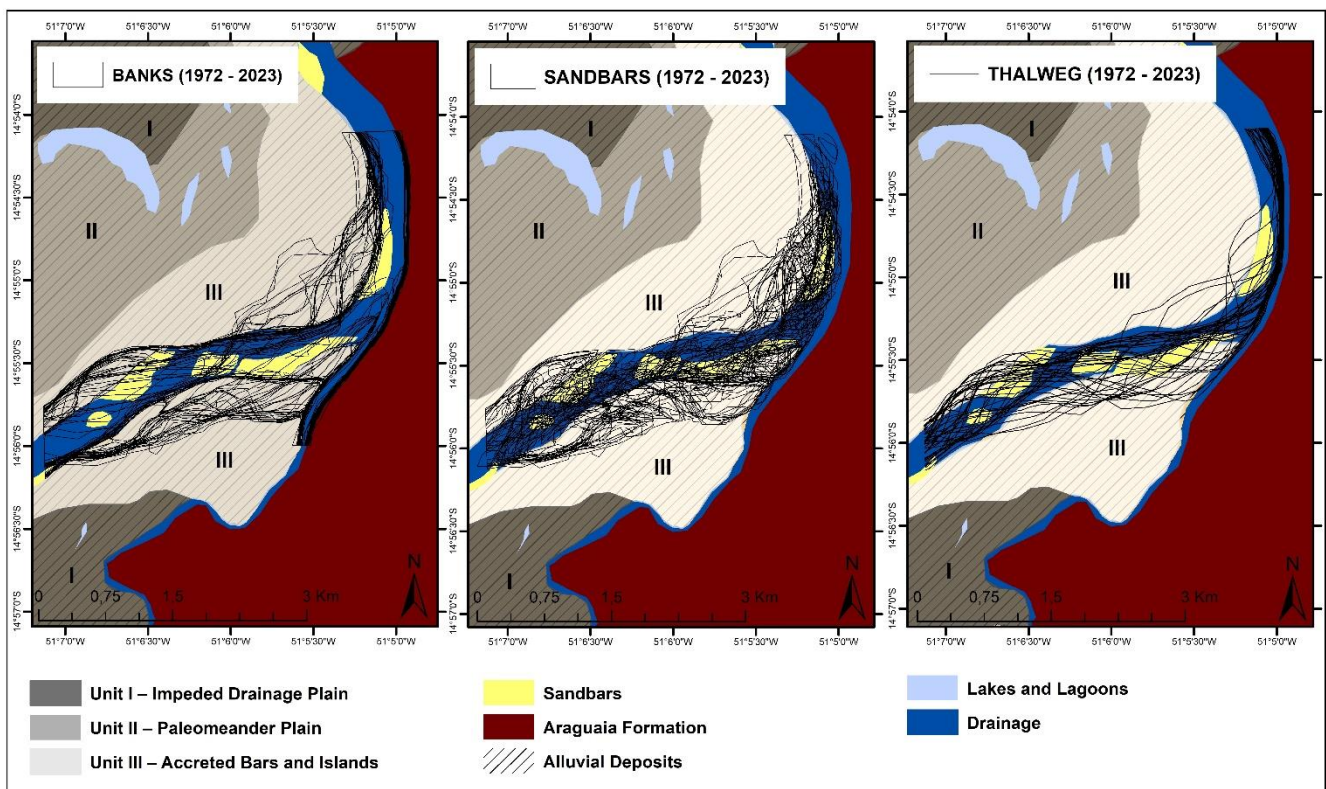


**Figure 13.** Geological and geomorphological characteristics at the Araguaia and Vermelho River confluence in 2023. Source: The authors, 2025.

As described by Dixon et al. (2018), confluences can achieve a greater degree of stability due to human interventions, especially by implementing containment structures along the banks. For example, the right bank of the stretch at the Araguaia and Vermelho River confluence is protected by such structures (Figure 14), which reinforce protection of this bank composed of the Araguaia Formation, where the urban area of the municipality of Aruanã is located. This human response to the mobility of confluences is also observed in the Padma and Meghna Rivers, in Bangladesh, and in the Yangtze and Dongting Rivers, in China (DIXON et al., 2018).



**Figure 14.** Containment structures at the Araguaia and Vermelho River confluence, from the right bank of the Vermelho River to downstream of the confluence. Source: The authors, 2025.

The stability of a river confluence can be sustained by several factors in addition to containment structures. Dixon et al. (2018) point out that many confluences of large rivers, such as the junctions between the Negro and Solimões Rivers in Brazil, maintain their location stable over decades. Although Franzinelli (2011) argues that the angle of this junction has undergone successive changes, evidenced by the formation and gradual transition of a set of fan-shaped river banks, Dixon et al. (2018) suggest that the Negro and Solimões River confluence has remained stable over the last 40 years.

The Congo and Kasai River confluence at Kwamouth in the Democratic Republic of the Congo is also characterized as stable due to the presence of bedrock, which prevents lateral migration of the channels. The Murray and Darling River confluence in New South Wales, Australia, exemplifies how climate change has resulted in reduced flows, decreasing channel size and lateral migration (NANSON et al., 2008; FITZSIMMONS et al., 2013). These effects were accentuated by interventions such as water diversions and the construction of dams (MAHESHWARI et al., 1995), in addition to implementing more than 3,600 reservoirs (ARTHINGTON; PUSEY, 2003). Although these confluences have maintained relative planimetric stability over the last four decades, the hydraulic processes that occur in them remain highly complex (DIXON et al., 2018).

This dynamism highlights the importance of investigating which processes influence confluence configuration over time. In this sense, Ettema (2008) highlights that understanding bank erosion and bar formation dynamics in confluence areas is essential, especially during extreme flood events, as these processes directly influence the morphological evolution of rivers. Previous studies, such as those by: Graf (1980), Petts (1984), Allen et al. (1989), Grant et al. (2003), Gilvear (2004), Petts and Gurnell (2005) and Phillips et al. (2005), show that erosion and depositional processes at river confluences promote lateral and longitudinal adjustments in their position. These adjustments were also observed by Dixon et al. (2018), who highlight the migratory dynamics of confluences over time and in different locations.

An example of this phenomenon occurs at the confluence of the Meta River (with a braided pattern) with the Orinoco River in Venezuela, where the junction migration is driven by bar dynamics. The high sediment production and water seasonality of the Meta River result in forming bars and islands which emerge during the low flow period (NORDIN; PEREZ-HERNANDEZ, 1989; DIXON et al., 2018), promoting migration of the confluence by approximately 1 km, both upstream and downstream.

Similarly, the Jamuna and Ganges River junction in Bangladesh is a notable example of a confluence influenced by channel migration, where confluence migration can reach distances of several kilometers in a single year, as described by Best and Ashworth (1997). The evolutionary response of a confluence to channel movement

is also observed in meandering rivers at the Paraguay and Bermejo River junction in Argentina. Although the Paraguay River is relatively stable in this section, the migration of meanders in the Bermejo River upstream of the confluence induces changes in its location. The confluence migrated approximately 600 m between 1985 and 2011, accompanied by a change in channel sinuosity (DIXON et al., 2018).

Another case occurs at the Mississippi and Arkansas River confluence in the USA, a highly dynamic junction in a meandering river. The migration of meanders associated with bar deposition, fixation and erosion resulted in displacement of the confluence by approximately 5 km (DIXON et al., 2018). Furthermore, at the Sarda and Ghaghara River confluence (the Ghaghara, a tributary of the Ganges) in Uttar Pradesh, northern India, the migration of the channel belt in its tributaries has led to junction displacement by about 22.7 km.

The Padma and Meghna River junction in Bangladesh has undergone a southward migration from the early 1970s to the mid-2000s, bringing the confluence closer to the city of Chandpur. Gazi et al. (2020) also documented the junction's migration over several kilometers. Finally, Wang and Xu (2020) investigated the Amite and Comite River confluence in Louisiana, USA, between 2002 and 2017. Their study revealed changes in the sedimentary bar formed at the junction, with the confluence migrating about 55 m over the analyzed period.

The results of this study also show that the high mobility of the channel and river landforms has resulted (and continues to result) in changes in the Araguaia and Vermelho River junction position, being in agreement with the data presented by Assis and Bayer (2020). They pointed out that there was a 424-meter retreat of the river junction between 1984 and 2018. This advance and retreat are more noticeable when analyzed based on section T4, which although did not present major changes in width between 1972 and 2023, it stood out as the most unstable among all the evaluated sections.

The changes observed in T4 are attributed to the confluence retreat as a result of the plain area erosion in this section. The retreat process can be observed from 1972 onwards, when the river junction was located 1.33 km downstream of section T4. The confluence began a process of progressive retreat between 1973 and 1994, but it still did not reach section T4. Then left bank of this section ceased to exist from 1995 onwards due to plain area erosion and consequently confluence retreat, being occupied at that time by the river area. The river junction in that year was located 200 m upstream of T4. However, it was not possible to measure the cross-section of T4 in the years 1995, 1996 and 1997 due to erosion of the left Vermelho Riverbank, since it was completely eroded, transforming it into an area occupied by water. The left bank of this section began to reestablish itself in 1998 with the formation of a tributary bar, thereby allowing this T4 section to be measured (with 67 m). This bar was eroded again in 1999, leading to an absence of the left bank of T4 again. A new tributary bar was formed from 2000 onwards and consolidated in the following years. This bar became part of the margin, gradually transforming into a plain area and contributing to advance the confluence.

The agreement between the results of both studies shows that advance and retreat dynamics make this confluence particularly susceptible to frequent changes in the junction angle and movement patterns. These phenomena directly reflect the influence of hydrosedimentological processes on confluence morphology. The junction angle plays an important role, influencing both the excavation zone morphology (MOSLEY, 1976; BEST, 1988; SAMBROOK SMITH et al., 2005) and the tributary bar formation and evolution (BEST, 1988).

A continuous change in the junction angle has been observed in response to channel mobility, fluvial geoforms and advance and retreat dynamics over the last 50 years at the Araguaia and Vermelho River confluence. The angle was 69.61° in 1972, decreasing to 42.30° in 2023, which represents a reduction of 27.31° in that period. Dixon et al. (2018) also identified changes in the angle of river junctions over 40 years. For example, there was a change in the angle at the Meta and Orinoco River confluence from 60° to 100°, while the Jamuna and Ganges River junction went from 70° to 100°.

The junction angles in Kurigram district, where three tributaries of the Jamuna River meet (the Gangadhar, Dud Kumar, and Dharla Rivers), varied from 30° to 80°, 30° to 70°, and 40° to 120°, as recorded by Dixon et al. (2018). A variation from 15° to 110° was also observed at the Paraguay and Bermejo River junction, and from 40° to 90° between the Mississippi and Arkansas Rivers. The junction angle at the Sarda and Ghaghara River confluence changed from 35° to 90°, while the change between the Padma and Meghna Rivers was from 15° to 90°. Wang and Xu (2020) investigated the confluence of the alluvial Amite and Comite Rivers from 2002 to 2017, and observed a reduction in the junction angle from 100° to 45°.

According to Best and Rhoads (2008), confluences with open angles (i.e. above 90°) promote greater deflection of the flow between the channels, thus altering the path of sediment transport. On the other hand, more closed

angles (smaller than  $90^\circ$ ) limit penetration of the bar at the confluence and favor advancing the bar towards the excavation zone, contributing to naturally fill this area. The confluence between the Araguaia and Vermelho Rivers falls into this second case, with the dominant frequency of the junction angle oscillating between  $40^\circ$  and  $75^\circ$ , but with a very high annual variation, especially since 1995 (Figure 10-B). Therefore, the results showed the excavation zone exhibiting repositioning trends (Figure 12 - T5), junction point migration (Figure 8), and the tributary bar area constantly increasing and decreasing in the same period (Figure 7).

The presence of this excavation zone in the central area of the confluence can be explained by several hydrodynamic and sedimentary factors already discussed in the literature. Among them, the accelerated flow in the central region of the confluence, the influence of turbulence along the shear layer between the flows, the action of secondary flows which affect the channel bed, and the sediment rotation process, which contributes to cleaning and maintenance of the excavated area, as pointed out by Atkinson (1987) and Roy and Bergeron (1988). These dynamics corroborate the morphological patterns described in classic studies by Mosley (1976), Best (1987, 1988), Biron et al. (1993) and Rhoads and Kenworthy (1995).

Channel adjustment mechanisms, which include erosion, deposition, and changes in the thalweg, impact several parameters of the hydraulic geometry of the Araguaia River in the study area. This dynamic has also been observed in previous studies (GRAF, 1980; PETTS, 1984; ALLEN et al., 1989; GRANT et al., 2003; GILVEAR, 2004; PETTS and GURNELL, 2005; PHILLIPS et al., 2005). An example of this process is the variation in width, depth, and velocity between T1 and T2 cross-sections resulting from development of the tributary bar on the right bank of T2 (Figure 15). This configuration promotes flow confinement in a narrow strip on the opposite side of the channel, resulting in higher velocity values in section T2 ( $0.623 \text{ m}\cdot\text{s}^{-1}$ ) compared to T1 ( $0.352 \text{ m}\cdot\text{s}^{-1}$ ) (Table 2).

At the same time, the development of the tributary bar shifts the thalweg to the left (Figure 5 B – Thaleg and Figure 12 – T2) and reduces the width of T1 (391.74 m) to T2 (290.4 m), and the average depth of T1 (1.46 m) to T2 (1.01 m). It is also noteworthy that development of the tributary bar in the Araguaia channel (section T2, Figure 15) is favored by the flow separation zone generated by the flow meeting which bypasses the right side of the central bar between the T1 and T2 sections. This contributes to deposition in the submerged portion of the tributary bar, reduced depth and the subsequent effects on the width and the thalweg.

It was not possible to establish the effect of these processes on the flow, although hydraulic geometry models demonstrate a generally proportional relationship between width and flow in river channels (STEVAUX; LATRUBESSE, 2017). The discrepancy in the flow rates observed in T1 ( $202.99 \text{ m}^3\cdot\text{s}^{-1}$ ) and T2 ( $184.87 \text{ m}^3\cdot\text{s}^{-1}$ ) is due to the fact that it was possible to perform the complete transverse profiling route (bank-to-bank) in T1 with the ADCP, while the submerged (very shallow) portion of the tributary bar in T2 prevented the complete route to obtain data (depth less than the minimum limit for the vessel and the ADCP).

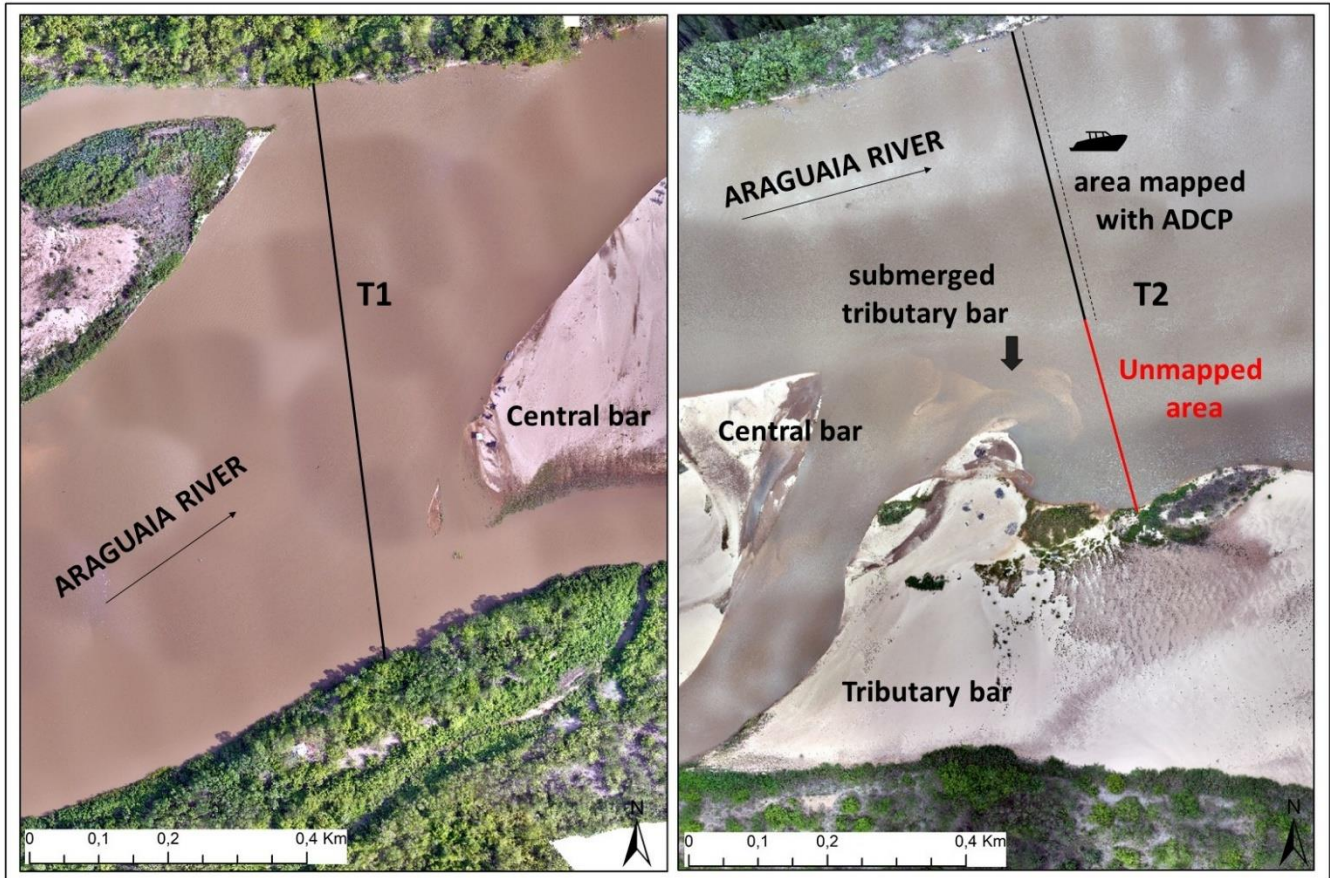


**Figure 15.** Details of the T1 and T2 cross-sections of the Araguaia River. Source: The authors, 2025.

The predominance of lateral bars over other types in the confluence region is in line with the representativeness of these bars in both quantity and area, as observed by Suizu et al. (2022) in their survey of other stretches of the Araguaia River. Some of these bars present relative stability when the adjustment mechanisms between the flow hydraulics and the erosion and deposition processes establish a local tendency for unidirectional thalweg displacement.

Mosley (1976) and Best (1988) discuss the formation of central bars in post-confluence channels. This type of bar was identified at the Araguaia and Vermelho River confluence in 1985, 1986, 1987, 1992, 1993, 1994, 1996, 1999, 2000, 2001, 2003, 2004, 2016, 2017, 2020 and 2021. This bar formation is related to the convergence of sediment transport paths (BEST, 1988; BEST; RHOADS, 2008), as well as to reduced flow velocities and a decrease in turbulence intensities immediately after the maximum flow acceleration zone (BEST, 1987; BEST, 1988; SUKHODOLOV; RHOADS, 2001; RHOADS; SUKHODOLOV, 2004).

### 5.2. Vegetation colonization and stabilization of the tributary bar

Variations in the total area of the lateral bars and in the tributary bar during the period analyzed at the Araguaia and Vermelho River confluence are directly related to the progressive ecological succession of riparian vegetation. This process resulted in converting extensive areas of sandy bars of the active channel into alluvial plain terrain (Figure 16). Consolidation of the tributary bar can be observed, which has been gradually incorporated into the right bank of the Araguaia River since 2002, as also observed by Assis and Bayer (2020).

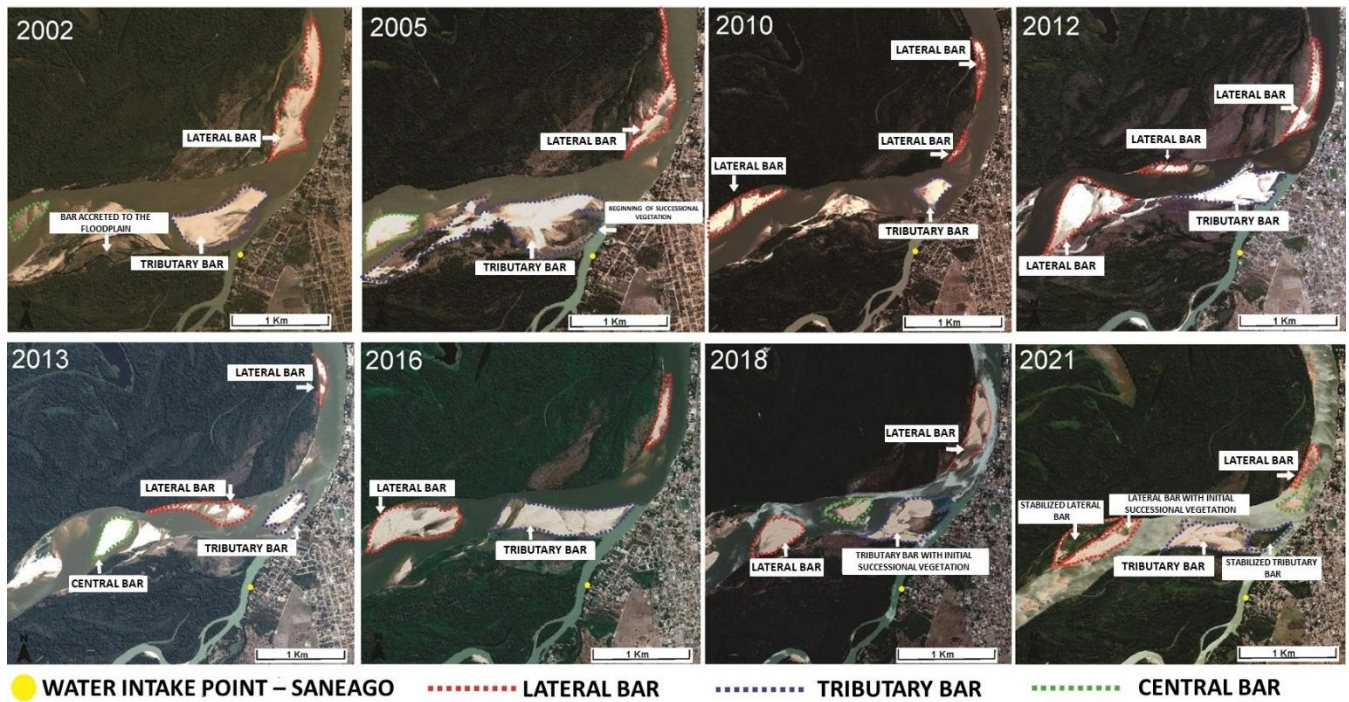


**Figure 16.** Conversion of lateral bars and tributary areas into floodplain lands by stabilization, plant colonization and bank attachment. Background images: Google Earth. Source: The authors, 2025.

This riparian vegetation which colonizes the river bars of the Araguaia River is classified as herbaceous pioneer vegetation, as defined by Morais (2006). It is directly influenced by the seasonal annual river regime of the Araguaia River and characterized by the presence of small plants spaced apart from each other with grasses and sedges, as described by Araújo (2002) (Figure 17 - E).

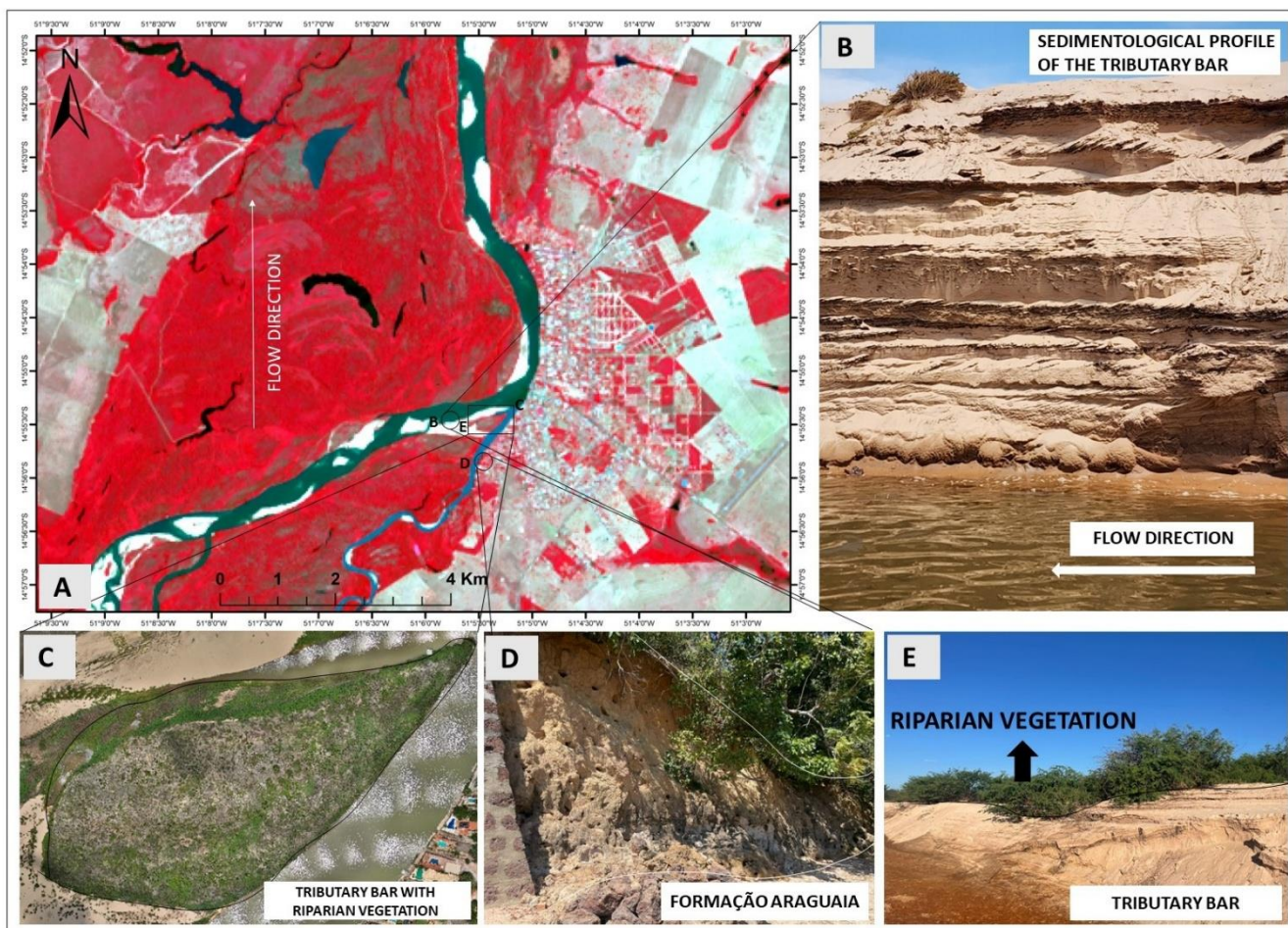


**Figure 17.** Examples of points indicating the different geological characteristics and consolidated vegetation at the Araguaia and Vermelho River confluence. (A) Landsat/OLI image from October 20, 2023, color composition R(5)G(4)B(3). (B) Sedimentological profile of the tributary bar in 2023 (with the presence of sand, silt and layer with organic material). (C) Riparian vegetation on the tributary bar. (D) Profile of the Araguaia Formation. (E) Example of riparian vegetation on the tributary bar. Photos: The authors, 2025.

The vegetation succession process in the region begins with establishment of herbaceous pioneer vegetation in small depression areas which are filled with clayey sediments rich in organic matter during floods. This is in line with the study by Wang and Xu (2020) and Assis and Bayer (2020), which indicate that the increase in the vegetated area in bars at the river junction is strongly related to flood events. These depressions favor rapid colonization of grasses, sedges, and some shrubs during droughts.

The accelerated growth of this vegetation allows these areas to remain preserved in the next hydrological cycles by forming a stabilizing cover which fixes the deposited material. This process not only facilitates consolidating sedimentary deposits, but also favors maintaining active areas over time. With succession, the vegetation becomes more resilient and capable of sustaining hydrological cycles, implying greater morphological stability in the region. This dynamic contributes to expanding deposition areas and plain construction in the long term, impacting the evolution of the river environment and forming new habitats (LATRUBESSE; STEVAUX, 2009; ASSIS, 2019; ASSIS e BAYER, 2020; SUIZU et al., 2022; SANTOS et al., 2024). This process has been one of the main factors responsible for consolidating the tributary bar, its annexation to the plain, and advancing the confluence over the last 20 years.

As discussed, the morphodynamics of confluences in floodplain areas, such as the Araguaia River, are especially sensitive to hydrosedimentary changes. Although this study provided a detailed analysis of the planimetric mobility and morphological reconfiguration of the Araguaia and Vermelho River confluence, there are

still gaps in knowledge about the geomorphological interactions at river confluences, especially in the context of the Cerrado Biome. Questions such as the influence of seasonal variations on sedimentation patterns, the transport of suspended and bottom sediments, as well as the role of pioneer vegetation in consolidating sandbanks and plain construction still require further investigation.

This investigation represents the first analysis focused on the morphology and fluvial dynamics of a confluence on the Araguaia River, integrating a detailed temporal analysis with data obtained by ADCP and echo sounder. The results highlight the need to expand this approach to other confluences of important tributaries, such as the Caiapó, Claro, Peixe, Crixás-Açu, Formoso, Côco, Piranhas, Cristalino and Rio das Mortes Rivers. An evaluation of confluences along the upper, middle and lower basins can also provide a comprehensive perspective on the hydrosedimentary and morphodynamic processes of this alluvial river. Incorporating mathematical and computational modeling emerges as an essential advance for deepening these analyses. The use of sediment transport simulation models, such as HEC-RAS and TELEMAC, can improve understanding of the geomorphological evolution of confluences under different hydrodynamic scenarios, increasing the applicability of the results.

## 6. Conclusion

This study analyzed the main morphological changes at the Araguaia and Vermelho River confluence located in the main river of the Cerrado biome. These changes were based on the planimetric displacement of fluvial geoforms from satellite images and hydrodynamic and bathymetric data obtained by ADCP. The results demonstrated marked instability of the confluence between 1972 and 2023, with continuous transformations in the erosion and depositional processes, in the mobility of the banks and in reconfiguration of the sand bars in both typology and quantity. In addition, fluvial junction angle and position variations were identified, as well as the presence of an excavation zone with a tendency to reposition within the channel.

The channel mobility is associated with migration of bars and thalweg, colonization of the bars by vegetation and differential erosion of the banks conditioned by the morphosedimentary units of the alluvial plain. While Unit III favors erosion and depositional processes due to low cohesion of the sediments, the presence of the Araguaia Formation acts as a resistant boundary to lateral migration. The morphological response of the confluence reflects the interaction between the seasonal hydro-sedimentary regime and lithological heterogeneity of the banks, characterizing a dynamic fluvial environment subject to continuous lateral and vertical adjustments.

These results indicate that erosion processes prevailed at the confluence at the beginning of the agricultural frontier expansion in the Araguaia River basin during the 1970s and 1980s. However, there has recently been a significant increase in depositional processes related to the hydro-sedimentary regime over the last five decades. This has contributed to forming and consolidating the tributary bar, which has played the main role in advancing the confluence over the last 20 years.

These changes significantly impact this stretch of the Araguaia River, the last major river in the Cerrado still free of direct human intervention. The effects of these changes may extend beyond the channel's morphological configuration, affecting port infrastructure, urban areas, lands and riverside properties, in addition to compromising fundamental ecological aspects, water flow regulation, the protection of flooded areas which act to mitigate floods, and most importantly tourism, which is the main income source for the population of Aruanã.

In this context, it is essential to seek more sustainable alternatives which are compatible with preserving this important area of the Cerrado biome. The conclusions of this study should be incorporated into developing predictive models, providing support for planning and strategic decision-making aimed at conservation and sustainable development of the river basin.

**Authors contributions:** Conception, P.C.A.; methodology, P.C.A and L.F.S.; formal analysis, P.C.A., M.H.C.Z., and H.A.M.; research, P.C.A.; data preparation, P.C.A. and L.F.S.; manuscript writing, P.C.A., M.H.C.Z., and H.A.M.; revision, M.H.C.Z. and H.A.M.; resources, M.B.; supervision, M.H.C.Z. All authors have read and agreed to the published version of the manuscript.

**Financing:** This study was funded by the National Council for Scientific and Technological Development - CNPq (#422559/2021-0) and the Postgraduate Program in Environmental Sciences at the Federal University of Goiás (UFG).

**Acknowledgements:** The authors would like to thank the Coordination for the Improvement of Higher Education Personnel – Brazil (CAPES) for granting the doctoral scholarship to the first author, Pâmela Camila Assis, whose support was essential for developing this study. They would also like to thank the Image Processing and Geoprocessing Laboratory (Lapig) linked to the Institute of Socioenvironmental Studies of the Federal University of Goiás (UFG) and the Federal Institute of Goiás (IFG – Campus Goiânia) for loaning equipment. Finally, they would like to thank the reviewers and the editor for their contributions that improved the quality of this manuscript.

**Conflict of Interest:** The authors declare they have no conflicts of interest.

## References

1. ABRAHAMS, A. D.; CAMPBELL, R. N. Source and tributary-source link lengths in natural channel networks. **Geological Society of America Bulletin**, n. 87, v. 07, p. 1016-1020, 1976. DOI: 10.1130/0016-7606(1976)87<1016:SATLLI>2.0.CO;2
2. ABRAHAMS, A.D.; UPDEGRAPH, J. Some space-filling controls on the arrangement of tributaries in dendritic channel networks. **Water Resources Research**, n. 23, p. 489-495, 1987. DOI: 10.1029/WR023i003p00489
3. ALLEN, P. M.; HOBBS, R.; MAIER, N. D. Downstream impacts of a dam on a bedrock fluvial system, Brazos River, Central Texas. **Bulletin of the Association of Engineering Geologists**, v. 26, n. 02, p. 165-189, 1989. DOI: 10.2113/gsegeosci.xxvi.2.165
4. ANA - Agência Nacional de Águas. **Conjuntura dos recursos hídricos no Brasil: regiões hidrográficas brasileiras**. Edição Especial. Brasília - DF: ANA. 2015. Disponível em: [https://www.ana.gov.br/acoesadministrativas/cdoc/CatalogoPublicacoes\\_2015.asp](https://www.ana.gov.br/acoesadministrativas/cdoc/CatalogoPublicacoes_2015.asp), acessado em Setembro de 2024.
5. AQUINO, S.; LATRUBESSE, E. E.; SOUZA FILHO, E. E. Relações entre o regime hidrológico e os ecossistemas aquáticos da planície aluvial do rio Araguaia. **Acta Scientiarum. Biological Sciences**, v. 30, n. 04, p. 361-369, 2008. DOI: 10.4025/actasciobiols.v30i4.5866
6. AQUINO, S.; LATRUBESSE, E. M.; SOUZA FILHO, E. E. Caracterização hidrológica e geomorfológica dos afluentes da Bacia do Rio Araguaia. **Revista Brasileira de Geomorfologia**, v. 10, n. 1, p. 43-54, 2009. DOI: 10.20502/rbg.v10i1.116
7. AQUINO, S.; STEVAUX J. C.; LATRUBESSE, E. M. Regime hidrológico e aspectos do comportamento morfohidráulico do rio Araguaia. **Revista Brasileira de Geomorfologia**, v. 06, n. 02, p. 29-41, 2005. DOI: 10.20502/rbg.v6i2.49
8. ARAÚJO, F. R. **Controles abióticos da vegetação na planície aluvial do rio Araguaia**. Dissertação (Mestrado em Geografia) - Programa de Pós-Graduação em Geografia, Universidade Federal de Goiás, Goiânia. 2002.
9. ARTHINGTON, A. H.; PUSEY, B. J. Flow restoration and protection in Australian rivers. **River Research and Applications**, v. 19, n. 05-06, p. 377-395, 2003. DOI: 10.1002/rra.745
10. ASSIS, P. C.; BAYER, M. Análise multitemporal do sistema fluvial do rio Araguaia, Aruanã - Goiás, Brasil. **Elisée - Revista de Geografia da UEG**, v. 09, n. 02, p. 01-18, 2020.
11. ASSIS, P. C.; SILVA, A. P. M.; FARIA, K. M. S.; BAYER, M. Implicações das transformações no uso e cobertura da terra na gestão hídrica da bacia hidrográfica do rio Araguaia. **Revista Geotemas**, v. 15, p. 01-25, 2025. DOI: 10.33237/2236-255X.2025.6459
12. ASSIS, P.C. **Estimativa do volume de depósitos sedimentares com o uso de veículo aéreo não tripulado (VANT) – Confluência do rio Araguaia com o rio Vermelho, Aruanã - GO**. 2019. 20 f. Monografia (Trabalho de Conclusão de Curso em Ciências Ambientais) - Instituto de Estudos Socioambientais, Universidade Federal de Goiás, Goiânia, 2019.
13. ATKINSON, B.K. **Fracture Mechanics of Rock**. London: Academic Geology Series, Academic Press, 1987. DOI: 10.1016/C2009-0-21691-6
14. BAGNOLD, R. A. **An approach to the sediment transport problem from general physics**. Washington: U.S. Department of the Interior, 1966. (Geological Survey Professional Paper, v 422-I, p.01 – 43).
15. BAGNOLD, R. A. **Sediment discharge and stream power** – A preliminary announcement. Washington: USGS. Geological Survey Circular, v. 421, p. 01-28, 1960.
16. BAYER, M. **Diagnóstico dos processos de erosão/assoreamento na planície aluvial do rio Araguaia: entre Barra do Garças e Cocalinho**. 2002. 138 f. Dissertação (Mestrado em Geografia) - Programa de Pós-Graduação em Geografia, Universidade Federal de Goiás, Goiânia. 2002.
17. BAYER, M. **Dinâmica do transporte, composição e estratigrafia dos sedimentos da planície aluvial do Rio Araguaia**. 2010. 104 f. Tese (Doutorado em Ciências Ambientais) - Programa de Pós-Graduação em Ciências Ambientais, Universidade Federal de Goiás, Goiânia. 2010.
18. BAYER, M.; ASSIS, P. C.; SUIZU, T. M.; GOMES, M. C. Mudança no uso e cobertura da terra na bacia hidrográfica do rio Araguaia e seus reflexos nos recursos hídricos, o trecho médio do rio Araguaia em Goiás. **Revista Confins**, n. 48, 2020. DOI: 10.4000/confins.33972

19. BAYER, M.; ZANCOPE, M. H. C. Ambientes sedimentares da Planície aluvial do Rio Araguaia. **Revista Brasileira de Geomorfologia**, v. 15, n. 02, p. 203-220, 2014. DOI: 10.20502/rbg.v15i2.414
20. BEST, J. L. Flow dynamics at river channel confluences: implications for sediment transport and bed morphology. **Recent Developments in Fluvial Sedimentology**, v. 39, p. 27-35, 1987. DOI: 10.2110/pec.87.39.0027
21. BEST, J. L. Sediment transport and bed morphology at river channel confluences. **Sedimentology**, v. 35, n. 03, p. 481-498, 1988. DOI: 10.1111/j.1365-3091.1988.tb00999.x
22. BEST, J. L. The morphology of river channel confluences. **Progress in Physical Geography: Earth and Environment**, v. 10, n. 02, p. 157-174, 1986. DOI: 10.1177/030913338601000201
23. BEST, J. L.; ROY, A. G. Mixing-layer distortion at the confluence of channels of different depth. **Nature**, v. 350, p. 411-413, 1991. DOI: 10.1038/350411a0
24. BEST, J.; ASHWORTH, P. Scour in large braided rivers and the recognition of sequence stratigraphic boundaries. **Nature**, v. 387, p. 275-277, 1997. DOI: 10.1038/387275a
25. BEST, J.L.; RHOADS, B. L. Sediment transport, bed morphology and the sedimentology of river channel confluences. In: RICE, S. P.; ROY, A. G.; RHOADS, B. L. (Org.). **River confluence, tributaries and the fluvial network**. London: Jhon Wiley & Sons Ltd, 2008. p.45-72. DOI: 10.1002/9780470760383.ch4
26. BIRON, P.; ROY, A. G.; BEST, J. L.; BOYER, C. J. Bed morphology and sedimentology at the confluence of unequal depth channels. **Geomorphology**, v. 08, 115-129, 1993. DOI: 10.1016/0169-555X(93)90032-W
27. BRISTOW, C. S.; BEST, J. L.; ROY, A. G. Morphology and facies models of channel confluences. In: MARZO, M.; PUIGDEFÀBREGAS, C. (Org.). **Alluvial Sedimentation**. Oxford: Blackwell, 1993. p. 89-100. DOI: 10.1002/9781444303995.ch8
28. BRUNS, D. A., MINSHALL, G. W., CUSHING, C. E., CUMMINS, K. M., BROCK, J. T., VANNOTE, R. L. Tributaries as modifiers of the river Continuum concept: Analysis by polar ordination and regression models. **Archive Hydrobiologie**, n. 99, p. 208-220, 1984.
29. CASTRO, S. S. Erosão hídrica na alta bacia do rio Araguaia: distribuição, condicionantes, origem e dinâmica atual. **Revista do Departamento de Geografia**, v. 17, p. 38-60, 2005. DOI: 10.7154/RDG.2005.0017.0004
30. COE, M. T.; LATRUBESSE, E. M.; FERREIRA, M. E.; AMSLER, M. L. The effects of deforestation and climate variability on the streamflow of the Araguaia River, Brazil. **Biogeochemistry**, v. 105, n. 01, p. 119-131, 2011. DOI: 10.1007/s10533-011-9582-2
31. DIXON, S. J.; SAMBROOK, S. G. H.; BEST, J. L.; NICHOLAS, A. P.; BULL, J. M.; VARDY, M. E.; SARKER, M. H.; GOODBRED, S. The planform mobility of river channel confluences: Insights from analysis of remotely sensed imagery. **Earth-Science Reviews**, v. 176, p. 01-18, 2018. DOI: 10.1016/j.earscirev.2017.09.009
32. ETTEMA, R. Management of confluences. In: RICE, S. P.; ROY, A. G.; RHOADS, B. L. (Org.). **River confluences, tributaries and the fluvial network**. London: Jhon Wiley & Sons Ltd, 2008. p. 93-118. DOI: 10.1002/9780470760383
33. FITZSIMMONS, K. E.; COHEN, T. J.; HESSE, P. P.; JANSEN, J.; NANSON, G. C.; MAY, J.H.; BARROWS, T. T.; HABERLAH, D.; HILGERS, A.; KELLY, T.; LARSEN, J.; LOMAX, J.; TREBLE, P. Late Quaternary palaeoenvironmental change in the Australian drylands. **Quaternary Science Reviews**, v. 74, p. 78-96, 2013. DOI: 10.1016/j.quascirev.2012.09.007
34. FLINT, J. J. Tributaries arrangements in fluvial systems. **American Journal of Science**, v. 280, p. 26-45, 1980. DOI: 10.2475/ajs.280.1.26
35. FRANZINELLI, E. Características morfológicas da confl uência dos rios Negro e Solimões (Amazonas, Brasil). **Revista Brasileira de Geociências**, v. 41, n. 04, p. 587-596, 2011. DOI: 10.25249/0375-7536.2011414587596
36. FRANZINELLI, E. Características morfológicas da confluência dos rios Negro e Solimões (Amazonas, Brasil). **Revista Brasileira de Geociências**, v. 41, n. 04, p. 587-596, 2011.
37. FRIEND, P. F.; SINHA, R. Braiding and meandering parameters. In: BEST, J. L.; BRISTOW, C. S. (Eds.). **Braided Rivers**. Geological Society Special Publication, n. 75, p. 105-111, 1993. DOI: 10.1144/gsl.sp.1993.075.01.05
38. GAZI, M. Y.; ROY, H.; MIA, M. B.; Akhter, S. H. Assessment of Morpho-Dynamics through Geospatial Techniques within the Padma-Meghna and Ganges-Jamuna River Confluences, Bangladesh. **KN - Journal of Cartography and Geographic Information Article**, v. 70, p. 127-139, 2020. DOI: 10.1007/s42489-020-00051-2
39. GHOSH, S.; MISTRI, B. Hydrogeomorphic significance of sinuosity index in relation to river instability: a case study of Damodar River, West Bengal, India. **International Journal of Advanced Earth Science**, v. 01, n.0 2, p. 49-57, 2012.
40. GILVEAR, D. J. Patterns of channel adjustment to impoundment of the upper River Spey, Scotland (1942-2000). **River Research and Applications**, v. 20, p. 151-165, 2004. DOI: 10.1002/rra.741
41. GOMES, M. C.; SOUZA, A. C. R.; BAYER, M.; FARIA, K. M. S. Degradação da vegetação nativa e implicações sobre o regime hidrológico na bacia hidrográfica do rio Claro, sub-bacia do rio Araguaia (GO). **Geociências**, v. 41, n. 03, p. 559 - 568, 2022. DOI: 10.5016/geociencias.v41i03.15579

42. GRAF, W. L. The effect of dam closure on downstream rapids. **Water Resources Research**, v. 16, n. 01, p. 129-136, 1980.
43. GRANT, G. E.; SCHMIDT, J. C.; LEWIS, S. L. A geological framework for interpreting downstream effects of dams on rivers. **Water Science and Applications**, v. 07, p. 209-225, 2003. DOI: 10.1029/007WS13
44. HACKNEY, C.; CARLING, P. A. The occurrence of obtuse junction angles and changes in channel width below tributaries along the Mekong River, South-East Asia. **Earth Surface Processes and Landforms**, v. 36, n. 12, p. 1563-1576, 2011. DOI: 10.1002/esp.2165
45. KOMINECKI, A.; VESTENA, L. Morfologia de confluência fluvial de ângulo agudo em área de controle geológico, Guarapuava, Paraná. **Brazilian Journal of Development**, v. 07, n.01, p. 8000-8018, 2021. DOI: 10.34117/bjdv7n1-543
46. LATRUBESSE, E. M.; AMSLER, M. L.; MORAIS, R. P.; AQUINO, S. The geomorphologic response of a large pristine alluvial river to tremendous deforestation in the South American tropics: The case of the Araguaia River. **Geomorphology**, v. 113, n. 03-04, p. 239-252, 2009. DOI: 10.1016/j.geomorph.2009.03.014
47. LATRUBESSE, E. M.; STEVAUX, J. C. Geomorphology and environmental aspects of the Araguaia fluvial basin, Brazil. **Zeitschrift für Geomorphologie**, v. 129, p. 109-127, 2002.
48. LATRUBESSE, E.; STEVAUX, J. C.; SINHA, R. Tropical rivers. **Geomorphology**, v. 70, p. 187-206, 2005.
49. LATRUBESSE, E.M.; STEVAUX, J. C.; BAYER, M.; PRADO, R. The Araguaia-Tocantins Fluvial Basin. **Boletim Goiano de Geografia**, v. 19, n. 1, p.120-127, 1999. DOI: 10.5216/bgg.v19i1.15341
50. MAHESHWARI, B. L.; WALKER, K. F.; McMAHON, T. A. Effects of regulation on the flow regime of the River Murray, Australia. **Regulated Rivers: Research and Management**, v. 10, n. 01, p. 15-38, 1995. DOI: 10.1002/rrr.3450100103
51. MILLER, J. P. **High mountain streams: Effects of geology on channel characteristics and bed material** (Memoir 4, State Bureau of Mines and Mineral Resources). New Mexico Institute of Mines and Mining Technology, p. 397-410, 1958.
52. MORAIS, Roberto Prado de. **A planície aluvial do médio rio Araguaia: processos geomorfológicos e suas implicações ambientais**. Tese (Doutorado em Ciências Agrárias) - Universidade Federal de Goiás, Goiânia, 2006. 178p.
53. MORISAWA, M. Tectonics and geomorphic models. In: MELHORN, W. N.; FLEMAL, R. C.(edits.). **Theories of Landform Development**. London: G. Allen & Unwin, 1975. p. 199- 216.
54. MOSLEY, M. An experimental study of channel confluences. **The Journal of Geology**, v 84, n. 05, p. 535-562, 1976. DOI: 10.1086/628230
55. NANSON, G. C.; PRICE, D. M.; JONES, B. G.; MAROULIS, J. C.; COLEMAN, M.; BOWMAN, H.; COHEN, T. J.; PIETSCH, T. J.; LARSEN, J. R. Alluvial evidence for major climate and flow regime changes during the middle and late Quaternary in eastern central Australia. **Geomorphology**, v. 101, n. 01, p. 109-129, 2008.
56. NIMNATE, P.; CHOOWONG, M.; THITIMAKORN, T.; HISADA, K. Geomorphic criteria for distinguishing and locating abandoned channels from the upstream part of Mun River, Khorat Plateau, northeastern Thailand. **Environmental Earth Sciences**, v. 76, n. 331, p. 01-13, 2017. DOI: 10.1007/s12665-017-6657-y
57. NORDIN, C. F.; PEREZ-HERNANDEZ, D. **Sand waves, bars, and wind-blown sands of the Rio Orinoco, Venezuela and Colombia**. Denver: US Geological Survey, 1989.
58. OLIVEIRA, A. S. **Análise morfométrica e granulométrica dos sedimentos transportados pelos rios Vermelho e Araguaia (confluência em Aruanã)**. 2021. 13 f. Monografia (Trabalho de Conclusão de Curso em Ciências Ambientais) - Instituto de Estudos Socioambientais, Universidade Federal de Goiás, Goiânia, 2021.
59. PETTS, G. E. **Impounded rivers: perspective for ecologia management**. Western Europe. Chichester: John Willey & Sons, 1984. DOI: 10.1016/j.geomorph.2004.02.015
60. PETTS, G. E.; GREENWOOD, M. Channel changes and invertebrate faunas below Nant-y-Moch dam, River Rheidol, Wales, UK. **Hydrobiologia**, n. 122, p. 65-80, 1985. DOI: 10.1007/BF00018961
61. PETTS, G. E.; GURNELL, A. M. Dams and geomorphology: research progress and future directions. **Geomorphology**, v. 71, n. 01-02, p. 27-47, 2005. DOI: 10.1016/j.geomorph.2004.02.015
62. PHILLIPS, J. D.; SLATTERY, M. C.; MUSSELMAN, Z. A. Channel adjustments of the lower Trinity River, Texas, downstream of Livingston Dam. **Earth Surface Processes and Landforms**, v. 30, n. 11, p. 1419-1439, 2005. DOI: 10.1002/esp.1203
63. RHOADS, B. L.; KENWORTHY, S. T. Flow structure at an asymmetrical stream confluence. **Geomorphology**, v. 11, n. 04, p. 273-293, 1995. DOI: 10.1016/0169-555X(94)00069-4
64. RHOADS, B. L.; SUKHODOLOV, A. N. Spatial and temporal structure of shear layer turbulence at a stream confluence. **Water Resources Research**, v. 40, n. 06, p. 01-13 2004. DOI: 10.1029/2003WR002811
65. RIBEIRO, M. L.; BLANCKAERT, K.; ROY, A. G.; SCHLEISS, A. J. Flow and sediment dynamics in channel confluences. **Journal of Geophysical Research: Earth Surface**, v. 117, n. 01, 2012. DOI: 10.1029/2011JF002171

66. RICE, S. P.; KIFFNEY, P.; GREENE, C.; PESS, G. R. The ecological important of tributaries and confluences. In: RICE, S. P.; ROY, A. G.; RHOADS, B. L. (Org.). **River confluences, tributaries and the fluvial network**. London: Jhon Wiley & Sons Ltd, 2008. v. 01, p. 209-242.
67. ROY, A. G.; ROY, R.; BERGERON, N. Hydraulic geometry and changes in flow velocity at a river confluence with coarse bed material. **Earth Surface Processes and Landforms**, n. 13, v. 07, p. 583-598, 1988. DOI: 10.1002/esp.3290130704
68. SAMBROOK SMITH, G. H.; ASHWORTH, P.; BEST, J. L.; WOODWARD, J.; SIMPSON, C. J. The morphology and facies of sandy braided rivers: some considerations of scale invariance. In: BLUM, M.; MARRIOTT, S.; LECLAIR, S. (Ed.). **Fluvial sedimentology**. 7. ed. Oxford: Blackwell Publishing, 2005. p. 145-158.
69. SANTOS, D. A. R.; CREMON, É. H.; CHEREM, L. F. S. Tendências temporais nas barras arenosas e massas de água na borda direita da maior ilha fluvial do mundo - rio Javaés. **Revista Brasileira de Geomorfologia**, v. 25, n. 01, p. 01-27, 2024. DOI: 10.20502/rbgeomorfologia.v25i1.2427
70. SANTOS, V. C.; STEVAUX, J. C. Processos fluviais e morfologia em confluências de canais: uma revisão. **Revista Brasileira de Geomorfologia**, v. 18, n. 01, p. 03-17, 2017. DOI: 10.20502/rbg.v18i1.1042
71. SEMAD - Secretaria do Meio Ambiente, dos Recursos Hídricos. Proposta de instituição do comitê da bacia hidrográfica do Rio Vermelho, conforme resolução nº 003, de 10 de abril de 2001, do Conselho Estadual de Recursos Hídricos. 2021. Disponível em: <https://goias.gov.br/meioambiente/wp-content/uploads/sites/33/2015/11/cbh-rio-vermelho-proposta-de-instituicao-b74.pdf>, acessado em Setembro de 2024.
72. SERRES, B.; ROY, A. G.; BIRON, P. M.; BEST, J. L. Three-dimensional structure of flow at a confluence of river channels with discordant beds. **Geomorphology**, v. 26, n. 04, p. 313-335, 1999. DOI: 10.1016/S0169-555X(98)00064-6
73. SILVA, P. R. F. **A expansão agrícola no cerrado e seus impactos no ciclo hidrológico: estudo de caso na região do MATOPIBA**. 2020. 156 f. Dissertação (Mestrado em Desenvolvimento Sustentável) - Universidade de Brasília, Brasília, 2020.
74. SOUZA et al. Reconstructing Three Decades of Land Use and Land Cover Changes in Brazilian Biomes with Landsat Archive and Earth Engine. **Remote Sensing**, v. 12, n 17, 2020. DOI: 10.3390/rs12172735
75. STEVAUX, J. C.; LATRUBESSE, E. M. **Geomorfologia fluvial**. São Paulo: Oficina de Textos, 2017. 336p.
76. SUIZU, T. M.; LATRUBESSE, E. M.; STEVAUX, J. C.; BAYER, M. Resposta da morfologia do médio-curso superior do Rio Araguaia às mudanças no regime hidrossedimentar no período 2001-2018. **Revista Brasileira de Geomorfologia**, v. 23, n. 02, p. 1420-1434, 2022. DOI: 10.20502/rbg.v23i2.2088
77. SUKHODOLOV, A. N.; RHOADS, B. L. Field investigation of three-dimensional flow structure at stream confluences: 2. Turbulence. **Water Resources Research**, v. 37, n. 9, p. 2411-2424, 2001. DOI: 10.1029/2001WR000317
78. VALENTE, C.R.; LATRUBESSE, E.M. Fluvial archive of peculiar avulsive fluvial patterns in the largest Quaternary intracratonic basin of tropical South America: The Bananal Basin, Central-Brazil. **Palaeogeography, Palaeoclimatology, Palaeoecology**, v 356-357, p. 62-74, 2012. DOI: 10.1016/j.palaeo.2011.10.002
79. WANG, B.; XU, Y. J. Decadal and episodic changes in morphology and migration of the confluence bar of two alluvial rivers in Louisiana, USA. **Journal of the American Water Resources Association**, v. 56, n. 04, p. p. 615-629, 2020. DOI: 10.1111/1752-1688.12838
80. ZANCOPE, M. H. C.; GONÇALVES P.E.; BAYER, M. Potencial de transferência de sedimentos e suscetibilidade á assoreamento na rede hidrográfica do Alto Rio Araguaia. **Boletim Goiano de Geografia**, v. 35, n. 01, p. 115-132, 2015. DOI: 10.5216/bgg.v35i1.35488



This work is licensed under the Creative Commons License Attribution 4.0 Internacional (<http://creativecommons.org/licenses/by/4.0/>) – CC BY. This license allows for others to distribute, remix, adapt and create from your work, even for commercial purposes, as long as they give you due credit for the original creation.